An Investigation on the Hydrogen gas sensitivity of Silicon Nanowire devices

By

Afrida Arshad

Urmila Saha

&

Sharmin Shoma

Submitted to the

Department of Electrical & Electronic Engineering

East West University

In partial fulfillment of the requirements for the degree of

Bachelor of Science in Electrical & Electronic Engineering

(B.Sc. in EEE)

Summer 2018

Thesis Advisor	Department Chairperson
Dr. Mohammad Mojammel Al Hakim	Dr. Mohammad Mojammel Al Hakim

Abstract

In this work we investigate feasibility of SiNW for hydrogen gas sensing application. We have used 58μm long p-type silicon NW with source and drain doping $10^{20}/cm^3$ and body doping of $6 \times 10^{16}/cm^3$. This particular structure has been used to resemble fabricated NW platform that has been used to extract the surface states density of SiNW when exposure of H_2 gas with pressure of 0.5, 1.0 and 1.5 bar. It is found that 100nm thick SiNW can exhibit sensitivity of H_2 gas down to 2500 ppm, 800 ppm, and 100 ppm for pressures of 0.5, 1.0 and 1.5 bar respectively if H_2 is exposed on NW in natural ambient. If H_2 is exposed on NW in vacuum environment this sensitivity goes down to 200 ppm, 100 ppm, and below 50 ppm respectively for 0.5, 1.0 and 1.5 bar. With the reduction of NW thickness a significant improvement of H_2 sensitivity is observed. For 10nm thickness SiNW can exhibit sensitivity of H_2 gas down to 500 ppm, 400 ppm, and below 50 ppm for pressure of 0.5, 1.0 and 1.5 bar respectively in natural ambient and in vacuum environment this sensitivity goes down to 100 ppm, 100 ppm, and below 50 ppm respectively for 0.5, 1.0 and 1.5 bar.

Acknowledgement

First of all, we would like to thank our thesis supervisor Professor Dr. Mohammad Mojammel Al Hakim, Department of Electrical and Electronic Engineering of East West University (EWU), Dhaka, for his affectionate guidance and giving us the great opportunity to research on this interesting topic. Without his support we could not reach the current stage with this thesis. He continually provided us with invaluable knowledge throughout this research. We greatly appreciate his dedication and owe him lots of gratitude for guiding us with friendly behavior.

We also want to thank to our honorable teacher Dr. Anisul Haque, Professor of Department of Electrical and Electronic Engineering of East West University for supporting us with his profound knowledge on semiconductor materials.

We are lucky that our supervisor and department chairperson both are same. So we also want to thank our department chairperson Dr. Mohammad Mojammel Al Hakim for his effort in the management of quality education.

Finally, we want to thank our family for supporting us as well as thank to all of our friends for their endless love and support.

Approval

The thesis title "An Investigation on the hydrogen gas sensitivity of silicon nanowire devices" submitted by Afrida Arshad (2014-1-85-016), Urmila Saha (2014-1-80-036) and Sharmin Shoma (2014-2-80-012) in the semester of Summer-2018, has been approved as satisfactory in partial fulfillment of the degree of the Bachelor of Science in Electrical and Electronic Engineering on August, 2018.

_____

Professor Dr. Mohammad Mojammel Al Hakim

Department of Electrical and Electronic

Engineering East West University, Dhaka 1212,

Bangladesh

Authorization

We hereby declare that we are the sole authors of this thesis. We authorize East West University to lend this thesis to other institutions for the purpose of scholarly research.

_____

Afrida Arshad

_____

Urmila Saha

_____

Sharmin Shoma

We further authorize East West University to reproduce this thesis by photocopy or other means, in total or in part, at the request of other institutions or individuals for the purpose of scholarly research.

_____

Afrida Arshad

_____

Urmila Saha

_____

Sharmin Shoma

Contents

Abstract 2
Acknowledgement 3
Approval 4
Authorization 5
List of Figures 7
List of Tables 8
Chapter 1 9
1.1 Introduction 9
1.2 Gas sensors and their applications 9
1.3 Gas sensitivity 10
1.4 Toxic gas and their effect on health and environment 10
1.4.1 Ammonia NH3 10
1.4.2 Sulfur dioxide SO2 11
1.4.3 Nitrogen dioxide NO2 11
1.4.4 Carbon Dioxide CO2 12
1.4.5 Carbon monoxide CO 12
1.4.6 Hydrogen gas H2 12
1.5 Conventional gas sensors 13
1.5.1 IR Detector 13
1.5.2 UV Detectors 14
1.5.3 Gas Chromatography 14
1.5.4 Metal Oxide Gas Sensors 14
1.5.5 Metal Oxide Nanowires 15
1.5.6 Silicon Nanowire based Sensors 15
1.6 Thesis motivation 16
1.7 Thesis organization 16
Chapter 2 17
Methodology of Simulation 17
2.1 Device features and models 17
2.2 Simulation Profile 18
Chapter 3 20
Results & Discussion 20
Chapter 4 33
Conclusion 33
References 34
Appendix A 35

List of Figures

Figure 2.1: Schematic Diagram of the Simulated p-type SiNW.....17
Figure 2.2: The distribution of acceptor and donor-like trap states across forbidden energy gap.....18
Figure 2.3: Cross-sectional view of p-type nanowire showing the mesh density in simulation 19
Figure 3.1: $Id\ vs\ Vg$ of 75nm thick NW at different concentration of $H2$ gas when $H2$ is exposed in air ambient 20
Figure 3.2: Relative Conductance Change (%) of 75nm nanowire at different concentration of $H2$ gas when $H2$ is exposed in air ambient 21
Figure 3.3: $Id\ vs\ Vg$ of 75nm thick NW at different concentration of $H2$ gas when $H2$ is exposed in vacuum ambient.....22
Figure 3.4: Relative Conductance Change (%) of 75nm nanowire at different concentration of $H2$ gas when $H2$ is exposed in vacuum ambient.....23
Figure 3.5: $Id\ vs\ Vg$ of 10nm thick NW at different concentration of $H2$ gas when $H2$ is exposed in air ambient 24
Figure 3.6: Relative Conductance Change (%) of 10nm nanowire at different concentration of $H2$ gas when $H2$ is exposed in air ambient 25
Figure 3.7: $Id\ vs\ Vg$ of 10nm thick NW at different concentration of $H2$ gas when $H2$ is exposed in vacuum ambient.....25
Figure 3.8: Relative Conductance Change (%) of 75nm nanowire at different concentration of $H2$ gas when $H2$ is exposed in vacuum ambient.....26
Figure 3.9(a): Peak conductance change (%) with respect to air as a function of $H2$ concentration for nanowire with different thicknesses and for $H2$ concentration at 0.5 bar pressure 27
Figure 3.9(b): Peak conductance change (%) with respect to air as a function of $H2$ concentration for nanowire with different thicknesses and for $H2$ concentration at 1.0 bar pressure 28
Figure 3.9(c): Peak conductance change (%) with respect to air as a function of $H2$ concentration for nanowire with different thicknesses and for $H2$ concentration at 1.5 bar pressure 29
Figure 3.10(a): Peak conductance change (%) with respect to vacuum as a function of $H2$ concentration for nanowire with different thicknesses and for $H2$ concentration at 0.5 bar pressure 30
Figure 3.10(b): Peak conductance change (%) with respect to vacuum as a function of $H2$ concentration for nanowire with different thicknesses and for $H2$ concentration at 1.0 bar pressure 31
Figure 3.10(c): Peak conductance change (%) with respect to vacuum as a function of $H2$ concentration for nanowire with different thicknesses and for $H2$ concentration at 1.5 bar pressure 32

List of Tables

Table 1.1 some common diseases identified by volatile organic compounds 10

Chapter 1

1.1 Introduction

Rapid ongoing industrial developments and further quality of life improvements put a large demand on the sensitive and selective detection of molecules in the gas phase for environmental monitoring, process control and safety, and medical diagnostics purposes. Gas sensors also began to appear in the chemical industry, environmental pollution monitoring and the human health fields, for instance, in the detection of explosive gases in the hydrogen production industry and methane distribution networks, air-quality monitoring in urban areas, breathe analysis for traffic safety and non-invasive medical diagnostics. [1]

A gas detector is a device that detects the presence of gases in an area, often as part of a safety system. This type of device is important because there are many gases that can be harmful to organic life, such as humans and animals. Exposure to toxic gases can also occur in operations such as painting, fumigation, fuel filling, construction, excavation of contaminated soils, landfill operations, entering confined spaces, etc. Common sensors include combustible gas sensors, photo ionization detectors, infrared point sensor ultrasonic, electrochemical gas sensor and semiconductor sensors. All of these sensors are used for a wide range of applications and can be found in industrial plants, refineries, pharmaceutical manufacturing, fumigation facilities, paper pulp mills, aircraft and shipbuilding facilities, hazmat operations, waste-water treatment facilities, vehicles, indoor air quality testing and homes. [2]

1.2 Gas sensors and their applications

The sensorial perception of the surroundings is very important for the development of animal and human lives. Humans will respond differently to various smells like sour meat and rotten eggs to avoid the danger of in taking unhealthy foods. Nevertheless, the human olfactory system can only detect a few kinds of gases qualitatively. Thus, the detection of poisonous CO, explosive liquefied petroleum gas and other dangerous vapors will acquire the assist of modern sensor technology. And the ethanol sensors can take the place of traditional detection methods for finding out drunken drivers. Furthermore, some intrinsic correlations between breath odors and diseases can be utilized in medical diagnostics. In 1971, Pauling et al separated and quantitated 250 substances in human breath by gas-chromatograph method. The research of the relationship between human breath and disease diagnostics has attracted the research community since then. Some organic compounds for the identification of several common diseases are shown in Table1.1. The advantageous of non-invasive and convenient compared with traditional detecting approaches make gas sensors very promising [3].

Table 1.1 some common diseases identified by volatile organic compounds

Disease	Compounds
Asthma	Leukotrienes
Liver disease	Hydrogen disulfide, limonene
Non Cholestatic	Hydrogen disulfide,2-propanol
Breast cancer	Quinazolinone,1-phenyl-ethanone, Heptanal
Sleep apnea	Interleukin IL-6,8-isoprostane
Uremia/Kidney failure	Dim ethylamine, trim ethylamine
Diabetes	Acetone

1.3 Gas sensitivity

The sensitivity is often decided by two factors.

- The minimum concentration of a target gas that can be detected by a gas sensor

- The response: it is usually defined as, $Sg = \frac{Xg-Xa}{Xa}$ where, X_g is the tested response value in the target gas environment and Xa is the response value in air. The X can be current, resistance, impedance, etc.

Variety of gas detection equipment is often prompted by changes in gas detection technology. So that as new detection methods replace old ones, several "generations" of gas detection devices are deployed at a single facility. The use of different instruments may also reflect changing preferences or a desire to take advantage of innovative features in products newly introduced to the market. Implicit in this variety is the need to find solutions tailored for specific applications.

1.4 Toxic gas and their effect on health and environment

There are different types of toxic gas in our environment. Those toxic gases mainly produce because of some environmental changes and some reaction in industrial side and some exposure. Those gases have a bad effect on health care and environment. In this paper we try to represent an overview of some toxic gases and their bad effects. Some of common toxic gases are Ammonia(NH3), Sulfur Dioxide ($SO_{2)}$, Nitrogen dioxide (NO2), Carbon Dioxide (CO2), Carbon monoxide (CO), Hydrogen gas (H2)etc.

Below there is a representation of their effects on health and environment:

1.4.1 Ammonia NH3

Ammonia (NH_3) is a colorless and pungent gas which is composed of nitrogen and hydrogen. Gaseous ammonia is continuously monitored in industrial refrigeration processes and biological degradation processes, including exhaled breath. Depending on the required sensitivity, different types of sensors are used Detectors usually operate near the lower

exposure limit of 25ppm. However, ammonia detection for industrial safety requires continuous monitoring above the fatal exposure limit of 0.1%.
People respond to chemical exposure in different ways. When ammonia enters into the body as a result of breathing, swallowing or skin contact, it reacts with water to produce ammonium hydroxide. This chemical reaction is very corrosive and damages cells in the body on contact. Exposure to high levels of ammonia in air may be irritating to your skin, eyes, throat, and lungs and cause coughing and burns. Lung damage and death may occur after exposure to very high concentrations of ammonia. Some people with asthma may be more sensitive to breathing ammonia than others.

When ammonia-based cleaners are drained down the sinks/toilets as a part of the housecleaning process, the waste treatment facilities are unable to remove ammonia before returning the water to rivers or lakes. This leads to the accumulation of ammonia in treated waters causing the rapid growth of some types of plants, that too in large numbers. When these plants die, they start decaying. This depletes the oxygen in the water, giving rise to algae. As a result, freshwater fish do not survive and their bodies too start decomposing. All these factors render the water useless for consumption, and even bathing. Air contamination due to ammonia released from industries and homes can contribute to smog.

1.4.2 Sulfur dioxide SO2

Sulfur dioxide (SO_2) is a colorless gas with a sharp, irritating odor. It is produced by burning fossil fuels and by the smelting of mineral ores that contain sulfur. Erupting volcanoes can be a significant natural source of sulfur dioxide emissions.

Sulfur dioxide is particularly harmful to the respiratory system's overall health. Likewise, the air pollutant is detrimental to both eye and skin health.SO2 is particularly dangerous for children. Studies correlate SO2 emissions from petroleum refineries even in lower exposure levels over time to higher rates of childhood asthma in children who live or attend school in proximity to those refineries. Sulfur dioxide irritates the respiratory tract and increases the risk of tract infections. It causes coughing, mucus secretion and aggravates conditions such as asthma and chronic bronchitis.

When sulfur dioxide combines with water and air, it forms sulfuric acid, which is the main component of acid rain. Acid rain can cause deforestation, acidify waterways to the detriment of aquatic life, and corrode building materials and paints. In Queensland, there is less heavy industry than in Europe or North America, where the potential for forming acid rain from sulfur dioxide emissions is higher. Our weather conditions and low sulfur content of fuels reduce the potential for acid rain.

1.4.3 Nitrogen dioxide NO2

Nitrogen dioxide is an irritating smelling gas. Some nitrogen dioxide is formed naturally in the atmosphere by lightning and some is produced by plants, soil and water. Nitrogen dioxide is a major air pollutant because it contributes to the formation of photochemical smog, which has significant impacts on human health.

The main effect of breathing in raised levels of nitrogen dioxide is the increased likelihood of respiratory problems. Nitrogen dioxide inflames the lining of the lungs, and it can reduce immunity to lung infections. This can cause problems such as wheezing, coughing, colds, flu and bronchitis. Increased levels of nitrogen dioxide can cause significant impacts on people

with asthma because it can cause more frequent and more intense attacks. Children with asthma and older people with heart disease are most at risk.

High levels of NO2 can have a negative effect on vegetation, including leaf damage and reduced growth. It can make vegetation more susceptible to disease and frost damage. A study of the effect of nitrogen dioxide and ammonia (NH3) on the habitat of Epping Forest has revealed that pollution is likely to be significantly influencing ecosystem health in the forest. The study demonstrated that local traffic emissions contribute substantially to exceeding the critical levels and critical loads in the area. The critical level for the protection of vegetation is 30 µg/m3 measured as an annual average. NO2 also reacts with other pollutants in the presence of sunlight to form ozone which can damage vegetation at high concentrations.

1.4.4 Carbon Dioxide CO2

Carbon dioxide is a colorless gas that contributes to global warming. It can also be a liquefied compressed gas or white flakes or cubes. In solid form, it is used as dry ice. Carbon dioxide is used for refrigeration, carbonation of beverages, and production of other chemicals, including methanol.

Carbon dioxide in its gas form is an asphyxiate, which cuts off the oxygen supply for breathing, especially in confined spaces. Exposure to concentrations of 10 percent or more of carbon dioxide can cause death, unconsciousness, or convulsions. Exposure may damage a developing fetus. Exposure can also cause dizziness, headache, sweating, fatigue, numbness and tingling of extremities, memory loss, nausea, vomiting, depression, confusion, skin and eye burns, and ringing in the ears.

For increase of 1 degree Celsius in temperature caused by carbon dioxide emissions, the resulting air pollution could lead to more than 20,000 deaths a year worldwide and many more cases of respiratory illness and asthma, a Stanford University study has found. CO2 has lots of effect on the environment like Rising Sea Level, Change of precipitation and local climate conditions; acid rain, Alteration of forests and crop yields, Expansions of deserts into existing rangelands, more intense rainstorms.

1.4.5 Carbon monoxide CO

Carbon monoxide is a colorless, nonirritating, odorless, and tasteless gas. It is found in both outdoor and indoor air. Carbon monoxide is made when carbon in fuel is not burned completely. Carbon monoxide in the air rapidly enters all parts of the body, including blood, brain, heart, and muscles when we breathe. Carbon monoxide can cause harm for heart, brain, and lungs. Breathing carbon monoxide during pregnancy can harm your unborn child. Carbon monoxide reacts with other pollutants in the air to form potentially harmful ground level ozone. This occurs close to the site of emission. It does not have any significant environmental effects at a global level.

1.4.6 Hydrogen gas H2

This is the first element in the periodic table. In normal conditions it's a colorless, odorless and insipid gas, formed by diatomic molecules, H_2. At normal temperature hydrogen is a not very reactive substance, unless it has been activated somehow; for instance, by an appropriate catalyzer. At high temperatures it's highly reactive. Extremely flammable, many reactions may cause fire or explosion. Gas/air mixtures are explosive. The substance can be absorbed into the body by inhalation. High concentrations of this gas can cause an oxygen-deficient

environment. Individuals breathing such an atmosphere may experience symptoms which include headaches, ringing in ears, dizziness, drowsiness, unconsciousness, nausea, vomiting and depression of all the senses. The skin of a victim may have a blue color at reactive hydrogen atmosphere. Under some circumstances, death may occur. Hydrogen is not expected to cause mutagen city, embryo toxicity, teratogenicity or reproductive toxicity. Pre-existing respiratory conditions may be aggravated by overexposure to hydrogen.

The gas mixes well with air, so explosive mixtures are easily formed. The gas is lighter than air. Heating may cause violent combustion or explosion. It reacts violently with air, oxygen, halogens and strong oxidants causing fire and explosion hazard. Metal catalysts, such as platinum and nickel, greatly enhance these reactions. High concentrations in the air cause a deficiency of oxygen with the risk of unconsciousness or death. Hydrogen forms 0.15 % of the earth's crust; it is the major constituent of water. 0.5 ppm of hydrogen gas and viral proportions as water vapors are present in the atmosphere. Hydrogen is also a major component of biomass, constituting the 14% by weight. Hydrogen occurs naturally in the atmosphere. The gas will be dissipated rapidly in well-ventilated areas. Any effect on animals would be related to oxygen deficient environments. No adverse effect is anticipated to occur to plant life, except for frost produced in the presence of rapidly expanding.

1.5 Conventional gas sensors

Nowadays the increasing concerns on the effects of pollution on health and for safety stress the need of real time monitoring of the environment, therefore there is a remarkable effort in terms of research for the development of sensors devoted to several applications.

1.5.1 IR Detector

The working principle of infrared gas detectors is based on the principle of infrared absorption. An infrared source illuminates the volume of a gas that has entered inside the measurement chamber. The gas absorbs some of the infrared wavelengths of 300nm as the light passes through it, while others pass through it completely not attenuated. The amount of absorption is related to the concentration of the gas and is measured by a set of optical detectors and suitable electronic systems. The change in the intensity of the absorbed light is measured relative to the intensity of light at a non-absorbed wavelength. The microprocessor computes and reports the gas concentration from the absorption. When there is no gas present the signals of reference signal detector and measurement signal detector are balanced. When there is combustible gas present, there is a predictable drop in the output from measurement signal detector because the gas is absorbing light. Their speed of response is very quick is which less than 10seconds [4]. They are immune to contamination and poisoning. If there is any failure of the source or blockage of the signal by dirt is detected as a malfunction.

Rich or poor environment infrared gas detectors are able to operate in oxygen but they are not able to detect gases which do not absorb energy. They are very big in size and cannot measure on the spot. Gas must cross the sampling path in order to be detected. Gases that do not absorb IR energy are not detectable. High humidity and dusty field environments can increase IR detection maintenance costs. A relatively large volume of gas is required to response testing. Ambient temperature of detector use is limited to 70℃. IR detectors does not perform well for multiple gas applications and cannot replace the IR source in the field, they must be returned to factory for repair.

1.5.2 UV Detectors

UV is the model used to describe the sensing mechanism which is based on the combination of the neck mechanism and grain boundary mechanism. We found that increasing the ultraviolet radiation flux density increases the conductivity of the film by decreasing the resistance. It has been experimented that due to incident UV radiation, it is possible to detect the gas sensitivity [5]. The effect of radiation on the sensitivity is discussed as a function of grain size and chemisorbed gas concentration.

1.5.3 Gas Chromatography

Gas chromatography is a chemical analysis instrument for separating chemicals in a complex sample. A gas chromatograph uses a flow-through narrow tube known as the *column*, through which different chemical constituents of a sample pass in a gas stream at different rates depending on their various chemical and physical properties and their interaction with a specific column filling, called the stationary phase. As the chemicals exit the end of the column, they are detected and identified electronically. The function of the stationary phase in the column is to separate different components, causing each one to exit the column at a different time. Other parameters that can be used to alter the order or time of retention are the carrier gas flow rate, column length and the temperature.

In Gas Chromatography analysis, a known volume of gaseous or liquid analytic is injected into the entrance of the column, usually using a micro syringe. As the carrier gas sweeps the analyte molecules through the column, this motion is inhibited by the adsorption of the analyte molecules either onto the column walls or onto packing materials in the column. The rate at which the molecules progress along the column depends on the strength of adsorption, which in turn depends on the type of molecule and on the stationary phase materials. Since each type of molecule has a different rate of progression, the various components of the analyte mixture are separated as they progress along the column and reach the end of the column at different times. A detector is used to monitor the outlet stream from the column; thus, the time at which each component reaches the outlet and the amount of that component can be determined. Generally, substances are identified by the order in which they emerge from the column and by the retention time of the analyte in the column.

Though gas chromatography need not large time for sensing they have some disadvantages too. The main disadvantage is that the substance to be chromatographed has to be volatile; it must vaporize within the temperature of the inlet. If any other object is injected, they will not vaporize, they will just decompose and really mess the inlet of the instrument. In GC, the column temperature can be changed but the mobile phase is always the same. It is highly specialized and cannot be used for any other gas mixtures.

1.5.4 Metal Oxide Gas Sensors

The conduct metric semiconducting metal oxide gas sensors currently constitute one of the most investigated groups of gas sensors. They have attracted much attention in the field of gas sensing under atmospheric conditions. In addition to the conductivity change of gas-sensing material, the detection of this reaction can be performed by measuring the change of capacitance, work function, mass, optical characteristics or reaction energy released by the gas or solid interaction [7]. This reaction can be influenced by many factors, including internal and external causes, such as natural properties of base materials, surface areas and microstructure of sensing layers, surface additives, temperature and humidity, etc. As one of the important parameters of gas sensors, sensitivity has been attracting more and more

attention and much effort has been made to enhance the sensitivity of gas sensors. There is not a uniform definition for gas sensor sensitivity now.

Though they have attracted much attention in the field of gas sensing they have some uncertainty too. They need very long time to detect gas sensitivity. The lifetime of the sensors made by metal oxide are very short and they need excess heat around 300℃.

1.5.5 Metal Oxide Nanowires

Metal oxide NW based chemical sensors have been investigated recently; their electrical conductivity varies with the composition of the surrounding gas atmosphere and metal oxides NWs like SnO2, TiO2, WO3, ZnO, Fe2O3 and In2O3 as well as the benefits from the addition of noble metals in improving selectivity and stability have been studied. In Nano sized grains almost all the carriers are trapped at surface states, the conduction is governed only by the few thermal activated carriers. When the metal oxide interacts with target gas species a transition form activated strongly to non-activated carrier density may occur with a huge effect on sensor conductance [8].

The successful synthesis of stable single crystal quasi-one-dimensional metal oxide nanostructures has been an unexpected breakthrough in many different fields that have not yet fulfilled all their promises. They are not selective yet and are of high power consumption. Concerning their use in chemical sensing; a significant improvement on the stability of the sensors platforms can be achieved using different sensing materials, but providing stable and reliable electrical contacts. The nanowires transfer and assembly by utilizing contact printing may enable the development of an all-printed technology for sensors that should achieve high performances, but maintaining low fabrication costs. Novel approaches such as self-heating and optical excitation significantly reduce the power consumption and allow a faster and reliable response even at room temperature. While the use of surface modification or other transduction principles like surface ionization and photoluminescence, with their considerably different response spectra, do increase their selectivity [8]. On top of all these efforts aimed at improving the performances of sensing materials, significant steps forward can be made with a constant effort in understanding the working principles which is the only way to guarantee the preparations of reliable, sensitive, selective and stable sensing materials and in turn sensor platforms. In spite of extensive activities worldwide in the research and development of these sensors, the basic scientific understanding of practically useful gas sensors is still poor.

1.5.6 Silicon Nanowire based Sensors

Nowadays, electrical devices made from SiNWs allow one to analyze responses not only by the voltage between the electrodes, but also by a gate voltage. Also, they have relative large carrier mobility and are tunable by controlling the doping level. Moreover, the fundamental sensor mechanism, gas sensors based on SiNWs are better understood than devices based on metal-oxide nanowires and polymer nanowires.

Penner wrote a review on chemical sensing with nanowires that includes relevant sections on SiNW based devices and also on examples of gas sensing. In 2007, Heath and co-workers reported a study on a NO2 sensor based on SiNWs, made by transferring hundreds of pre-aligned, top-down prepared SiNWs from a silicon-on-oxide (SOI) wafer onto plastic [1].

Reported studies suggest that gas sensing using conventional metal oxide film and nanoparticle based sensors in room temperature usually exhibit slow response/recovery times

due to inherent electron transfer mechanism and gas adsorption chemistry. Silicon nanowire based gas sensors are currently in interests due to its promise for fast response in room temperature. However, detection limit (gas sensitivity) and/or conductance change upon gas exposure, response/recovery times of silicon based sensors typically depend on material topology (i.e. pore diameter/pore density for porous silicon and nanowire density for bottom up grown or chemically etched nanowires etc.), nanowire dimension (i.e. diameter), doping density, surface stoichiometry/texture etc. Although porous silicon is believed to facilitate gas adsorption through randomly distributed pores, typical response time of porous silicon thin film sensors for different gases are around the order of several minutes. In order to achieve fast response utilizing high surface to volume ratio, silicon nanowires are recently researched as gas sensors and response/ recovery times are reduced to a value around 25 to 60 seconds for some gases [11].

1.6 Thesis motivation

Although SiNW just recently has been researched for gas sensing application the no. of reports are actually only a few. There is also no report available showing intrinsic H_2 gas sensitivity of SiNWs. In this work we perform flexibility of SiNW for gas sensing application by exploiting a target gas H_2, acknowledging the importance of H_2 gas sensor in industries.

1.7 Thesis organization

Chapter 1: provides related information about toxic gases which are harmful to the environment and health and their sensing technologies, also gas sensing devices which can detect them along with SiNW based devices. A few number of research papers related with SiNW was being studied.

Chapter 2: describes simulation methodology, simulation profile, along with required models for the simulation.

Chapter 3: describes the simulation results for nanowire thickness of 10nm and 75nm with length of 58μm. Also the result of H_2 concentration detected at different level of pressure in vacuum and air ambient.

Finally, in **Chapter 4** we summarize this work.

Chapter 2

Methodology of Simulation

2.1 Device features and models

The investigation on the hydrogen gas sensitivity of Silicon nanowire based devices were done with the help of numerical simulations using the software SILVACO Atlas device simulator [9], installed on the VLSI lab of East West University. A p-type silicon nanowire was created on 500nm nitride with a 500nm buried Si layer. A backgate is made with 20nm Al beneath the buried Si layer. In the silicon nanowire, two heavily doped regions on the two sides of the channel were employed to ensure ohmic contact on the source/drain regions. The source/drain regions were heavily doped with the doping density of $10^{20}/cm^3$. The whole NW was covered with 10nm oxide.

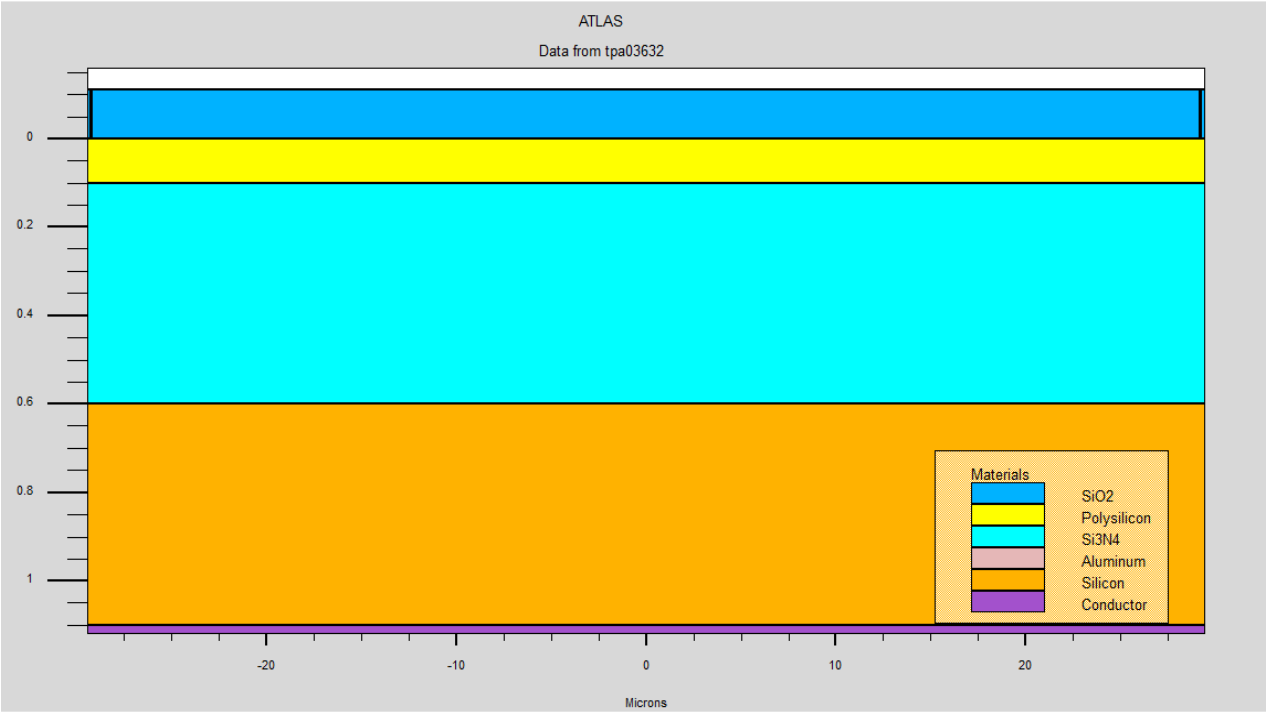

Figure 2.1: Schematic Diagram of the Simulated p-type SiNW

For simulation our Si NW thickness were chosen at 10nm, 25nm, 50nm, 75nm and 100nm. Body doping of NW was also varied from $10^{16}/cm^3$ to $10^{18}/cm^3$ as Si-NW thickness 10nm quantum effect is neglected and a classical drift diffusion model is used to investigate Si-NW behavior.

In our simulation Fermi-Dirac (FERMI) carrier statistics of Poisson's drift-diffusion solver was used to model carrier transport in poly silicon NW. The SRH (Shockley-Read-Hall) model for carrier emission and absorption was used to reflect the recombination phenomena within the device. SRH uses concentration dependent lifetimes.

The band gap narrowing effects in the heavily doped source/drain regions were included by Slotboom and de Graaff's analytical BGN model. However, for mobility we used constant

mobility model for poly silicon NWS simulation because TFT module in ATLAS is compatible with constant low field mobility model only.

We have used mobility of electron = 14cm^2/V.s and mobility of hole = 6cm^2/V.s in our simulation as experimentally extracted mobility of similar polysilicon nanowires were within the range of 6cm^2/V.s to 12cm^2/V.s considering variation of polysilicon nanowire width and height after fabrication.

Poly silicon is a disorder material which contains a large number of defects states within the band gap of the material and interface. The defect states as a combination of exponentially decaying band tail states and Gaussian distribution of mid gap states [9] shown in Figure 2.2. We therefore model the poly silicon using a continuum of trap states consist of both donor-like and acceptor-like states distribution across the energy band gap. The defect states as a combination of exponentially decaying band Tail states and Gaussian distribution of mid gap states are used with parameters previously used in the literature for successful modeling of poly silicon thin film transistor [10].

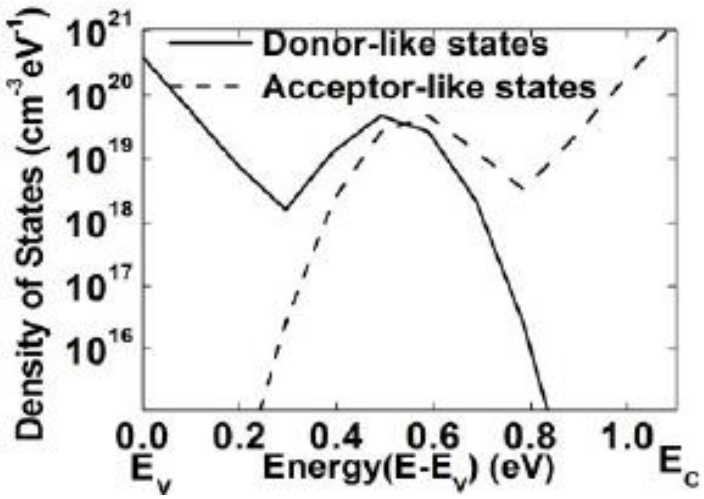

Figure 2.2: The distribution of acceptor and donor-like trap states across forbidden energy gap

2.2 Simulation Profile

Device simulation using SILVACO Atlas usually faces convergence problems and necessitates a long simulation run times. To avoid this problem at first, structure definition was performed. In this definition the simulation focused on creating the structure with a suitable mesh density. Regions and electrodes were defined as depicted in Figure 2.3. Finer nodes were assigned in critical areas, such as across the gate oxide to monitor channel activity and to get a better picture of the depletion layer and junction behavior near the source/drain boundaries. A coarser mesh was used elsewhere in order to reduce simulation run time. After specifying the doping the device is ready to simulation. Once the structure, mesh and doping were found to be as desired, the simulation was performed with appropriate models as discussed in section 2.1 and numerical solving methods.

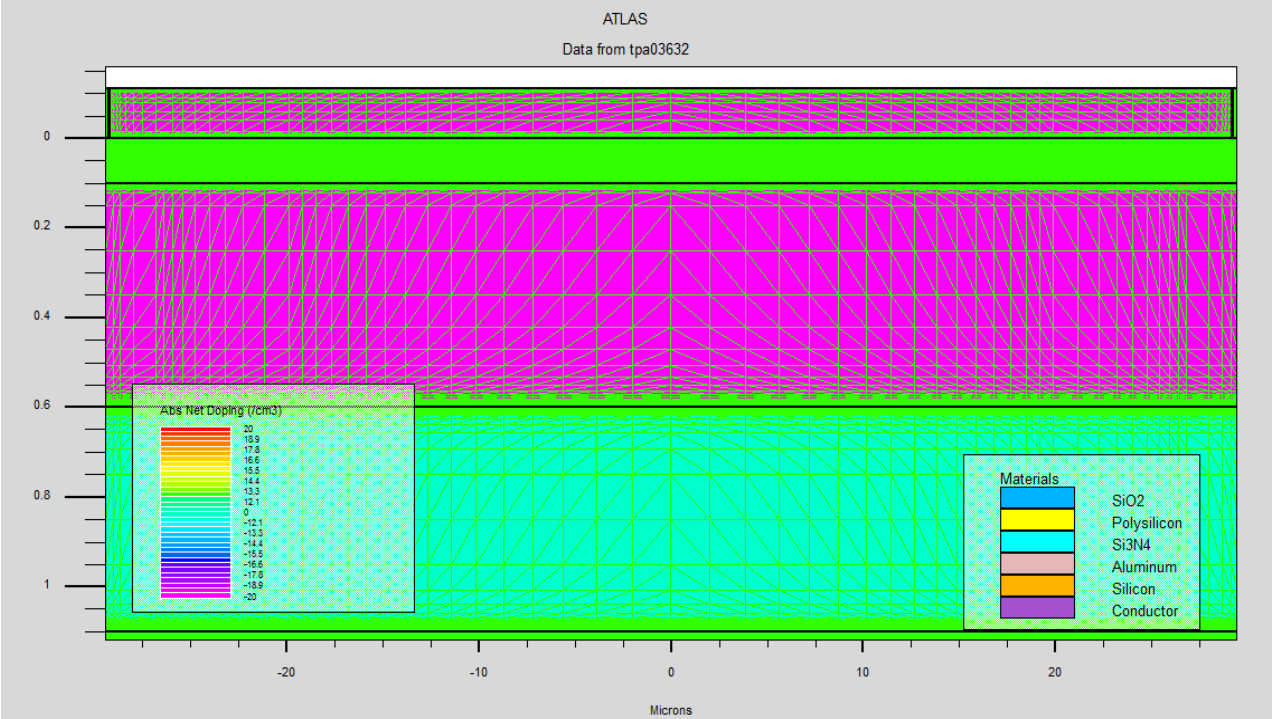

Figure 2.3: Cross-sectional view of p-type nanowire showing the mesh density in simulation

A special bias point solving method is use to get convergence, because the simulation faced difficulty in solving at the initial desired bias point. In our simulation the first initial drain bias point was 0.05v and the next bias point is 0.5v. Finally set the desired bias point for simulation.

Chapter 3

Results & Discussion

This chapter describes how H_2 gas sensitizes on SINW device. To investigate this issue we have taken p-type SiNW thickness of 10nm, 25nm, 50nm, 75nm, 100nm. We basically examined this issue on two states - air to H_2, vacuum to H_2. We observed this issue on different pressure of Hydrogen gas. The different pressure of Hydrogen gas is 0.5 bar, 1.0 bar, 1.5 bar. We not only observed this issue in different atmospheric pressure but also in different concentration of Hydrogen gas. The concentrations of Hydrogen gas are – 0.005%, 0.05%, 0.1%, 0.3%, 0.5%, 1%, 2%, 3%, 4%, and 5%. The whole investigation was basically done by observing sub threshold (Id vs. Vg) plot of these different states of Hydrogen gas and thickness of SINW and the peak change (%) of relative conductance.

The different exposure of H_2 gas introduces surface states in SiNW. So, when different concentration of H_2 gas is exposed on SiNW the amount of introduced surface states are extracted from reference [11]. This paper shows that for 100×100 nm NW for 5% H_2 exposure $5\times10^{10}/cm^2$, $1.4\times10^{11}/cm^2$ and $9.2\times10^{11}/cm^2$ number of states are introduced for the pressure of 0.5bar, 1.0bar and 1.5bar respectively. As 5% H_2 gas introduces such an amount of interface states we can readily calculate what will be the concentration of surface at other percentages and this simulation uses these experimentally calibrated surface states to find out the performance of SiNW at different H_2 concentration.

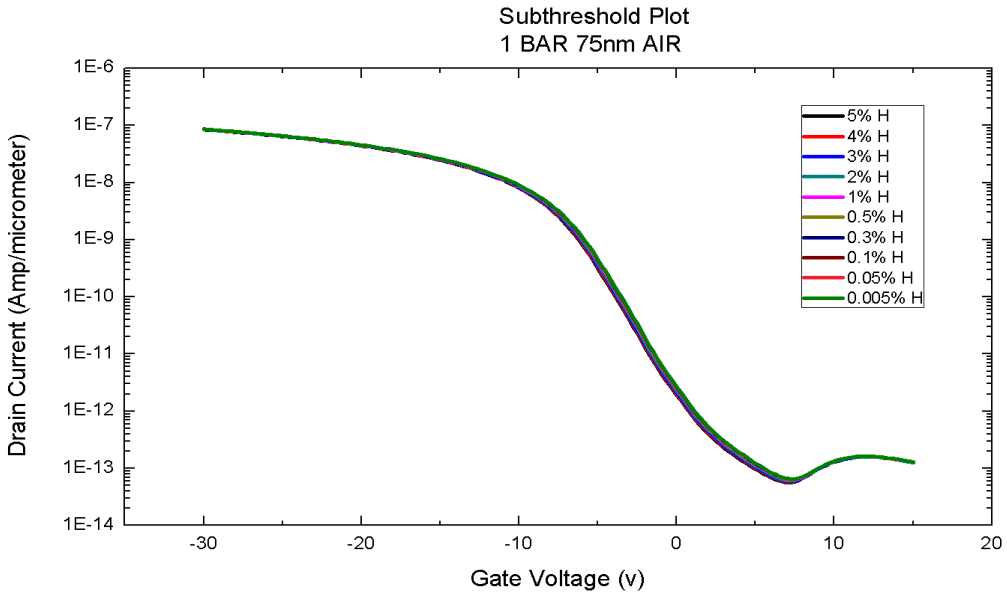

Figure 3.1: I_d vs V_g of 75nm thick NW at different concentration of H_2 gas when H_2 is exposed in air ambient

Figure 3.1 shows sub-threshold characteristics (I_{DS} vs. V_{GS}) of 58µm long p-type Si NWs for 75nm nanowire thickness in air ambient at different concentration of H_2 with pressure of Hydrogen gas 1bar. The drain to source voltage is 3.00v and gate to source voltage varies

from +15v to -30v. The drive current varies almost 2.40×10^{-12} $A/\mu m$ to 3.37×10^{-12} $A/\mu m$ for the change of concentration of hydrogen gas from 5% to 0.005% when gate to source voltage is -0.25v. If we focus on the drain current for gate voltage -30v the drain current varies from 8.45×10^{-08} $A/\mu m$ to 8.59×10^{-08} $A/\mu m$ for the concentration of hydrogen gas from 5% to 0.005%. It means if we decrease the concentration of hydrogen gas the drain current will increase.

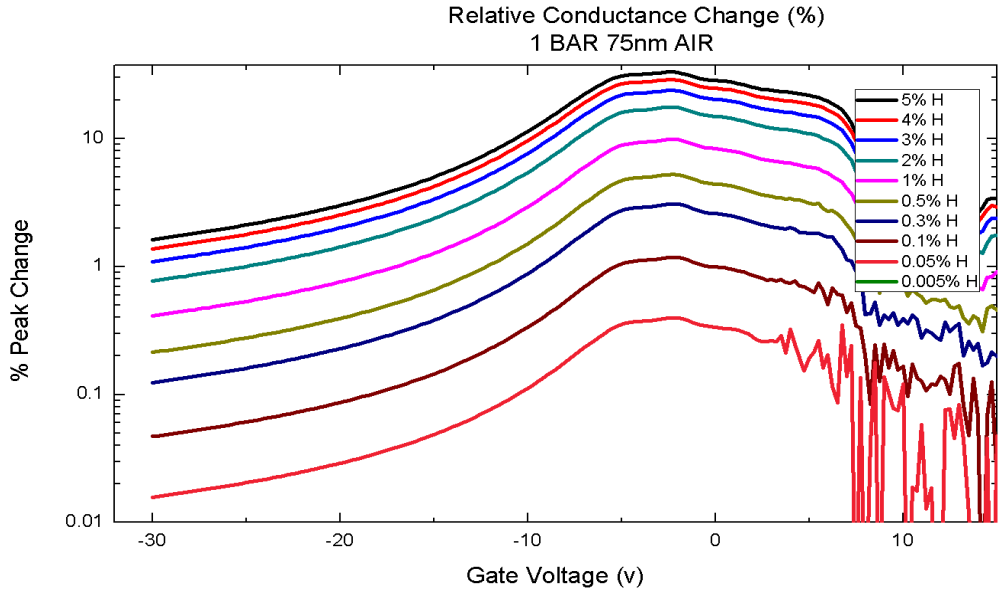

Figure 3.2: Relative Conductance Change (%) of 75nm nanowire at different concentration of H_2 gas when H_2 is exposed in air ambient

Figure 3.2 shows the relative conductance change (%) of 58µm long p-type Si NWs for 75nm nanowire thickness in air ambient at different concentration of H_2 with pressure of hydrogen gas 1bar. We compare all this donor state with standard air state where donor is 3×10^{11} to get the relative conductance change (%). The drain to source voltage is 3.00v and gate to source voltage varies from +15v to -30v.

By analyzing the data we get to know that along with the change of gate voltage from +15v to -31v the relative conductance change (%) at first increase and after passing the peak it started to decrease. If we focused on the figure the peak change (%) is almost at -2.25v gate voltage in air ambient. Along with the reduction of the concentration of gas the relative conductance also reduced its value for specific gate voltage.

Peak % change for 5% H_2 is 33.13329712 whereas for 0.005% is 0.

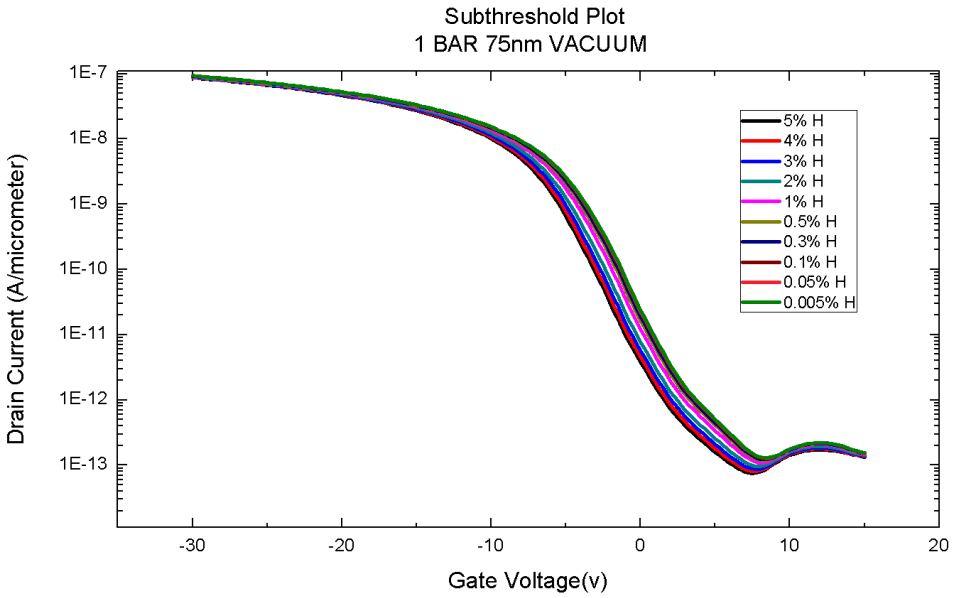

Figure 3.3: I_d vs V_g of 75nm thick NW at different concentration of H_2 gas when H_2 is exposed in vacuum ambient

Figure 3.3 shows sub-threshold characteristics (I_{DS} vs. V_{GS}) of 58µm long p-type Si NWs for 75nm nanowire thickness in vacuum ambient at different concentration of H_2 with pressure of hydrogen gas 1bar. The drain to source voltage is 3.00v and gate to source voltage varies from +15v to -30v. The drive current varies almost 4.80×10^{-12} $A/\mu m$ to 3.15×10^{-11} $A/\mu m$ for the concentration of hydrogen gas from 5% to 0.005% when gate to source voltage is -0.25v. If we focus on the drain current for gate voltage -30v the drain current varies from 8.73×10^{-08} $A/\mu m$ to 9.36×10^{-08} $A/\mu m$ for the concentration of hydrogen gas from 5% to 0.005%. It means if we decrease the concentration of hydrogen gas the drain current will increase.

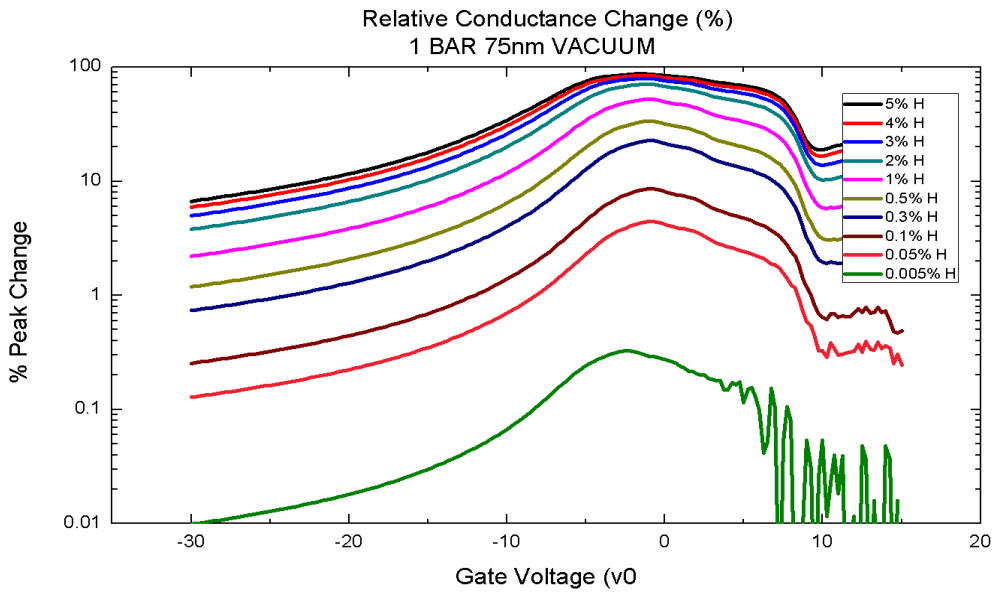

Figure 3.4: Relative Conductance Change (%) of 75nm nanowire at different concentration of H_2 gas when H_2 is exposed in vacuum ambient

Figure 3.4 shows the relative conductance change (%) of 58μm long p-type Si NWs for 75nm nanowire thickness in vacuum ambient at different concentration of H_2 with pressure of hydrogen gas 1bar. The drain to source voltage is 3.00v and gate to source voltage varies from +15v to -30v.

If we focused on the figure the peak change (%) is almost at -1.50v gate voltage in vacuum ambient. Peak % change for 5% H_2 is 87.27871644 whereas for 0.005% is 0.318652311 which demonstrates that NW would be more sensitive to H_2 gas if it is exposed in vacuum ambient.

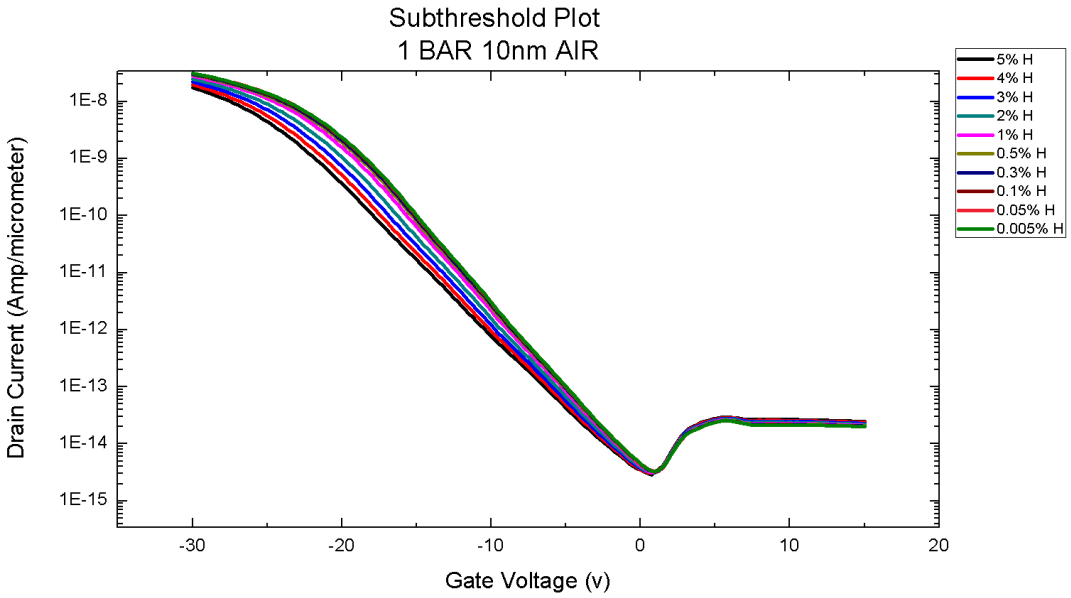

Figure 3.5: I_d *vs* V_g of 10nm thick NW at different concentration of H_2 gas when H_2 is exposed in air ambient

Figure 3.5 shows sub-threshold characteristics (I_{DS} vs. V_{GS}) of 58µm long p-type Si NWs for 10nm nanowire thickness in air ambient at different concentration of H_2 with pressure of hydrogen gas 1bar. The drain to source voltage is 3.00v and gate to source voltage varies from +15v to -30v. The drive current varies almost $3.72\times 10^{-15}\ A/\mu m$ to $5.20\times 10^{-15}\ A/\mu m$ for the concentration of hydrogen gas from 5% to 0.005% when gate to source voltage is -0.25v. If we focus on the drain current for gate voltage -30v the drain current varies from $1.75\times 10^{-08}\ A/\mu m$ to $3.12\times 10^{-08}\ A/\mu m$ for the concentration of hydrogen gas from 5% to 0.005%. It means if we decrease the concentration of hydrogen gas the drain current will increase.

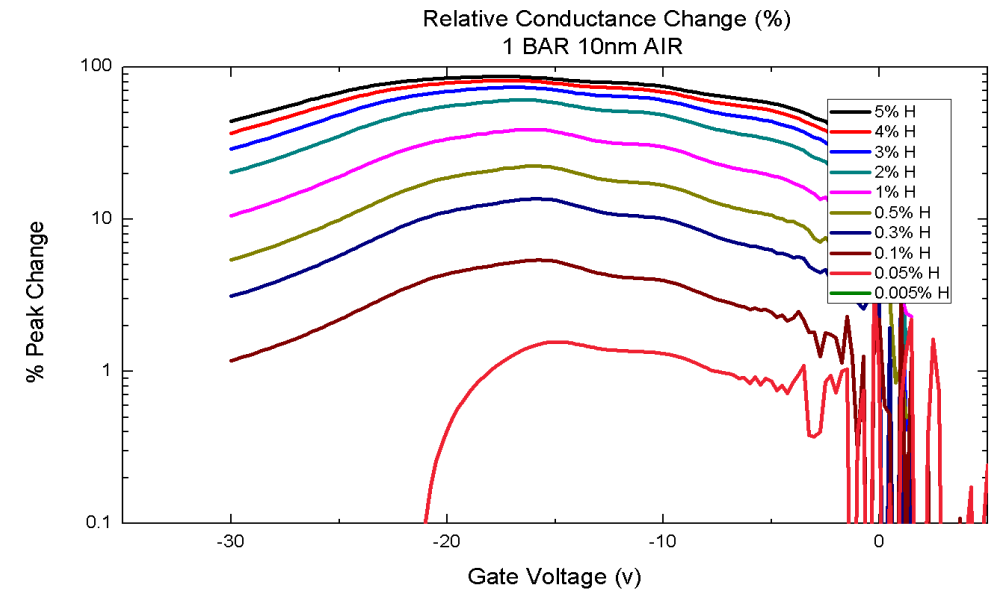

Figure 3.6: Relative Conductance Change (%) of 10nm nanowire at different concentration of H_2 gas when H_2 is exposed in air ambient

Figure 3.6 shows the relative conductance change (%) of 58µm long p-type Si NWs for 10nm nanowire thickness in air ambient at different concentration of H_2 with pressure of hydrogen gas 1bar. If we focused on the figure the peak change (%) is almost at -17.5v gate voltage in air ambient. Peak % change for 5% H_2 is 86.67498961 whereas for 0.005% is 0.

It is observed that 10nm thickness NW is more sensitive than 75nm thickness NW for H_2 gas exposure in air ambient.

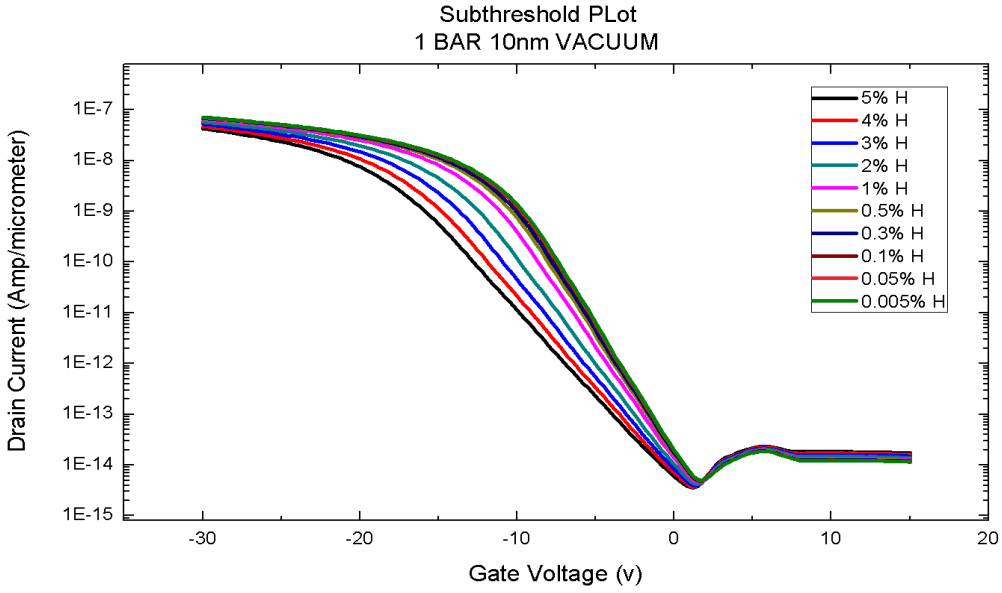

Figure 3.7: I_d vs V_g of 10nm thick NW at different concentration of H_2 gas when H_2 is exposed in vacuum ambient

Figure 3.7 shows sub-threshold characteristics (I_{DS} vs. V_{GS}) of 58µm long p-type Si NWs for 10nm nanowire thickness in vacuum ambient at different concentration of H_2 with pressure of hydrogen gas 1bar. The drain to source voltage is 3.00v and gate to source voltage varies from +15v to -30v. The drive current varies almost $7.03\times 10^{-15}\ A/\mu m$ to $2.60\times 10^{-14}\ A/\mu m$ for the concentration of hydrogen gas from 5% to 0.005% when gate to source voltage is -0.25v. If we focus on the drain current for gate voltage -30v the drain current varies from $4.25\times 10^{-08}\ A/\mu m$ to $7.16\times 10^{-08}\ A/\mu m$ for the concentration of hydrogen gas from 5% to 0.005%.

It is worth noting that change in the subthreshold characteristics for the change of H_2 gas concentration from 5% to 0.005% of 10nm NW in vacuum is much larger than 75nm in vacuum, 75nm in air, 10nm in air.

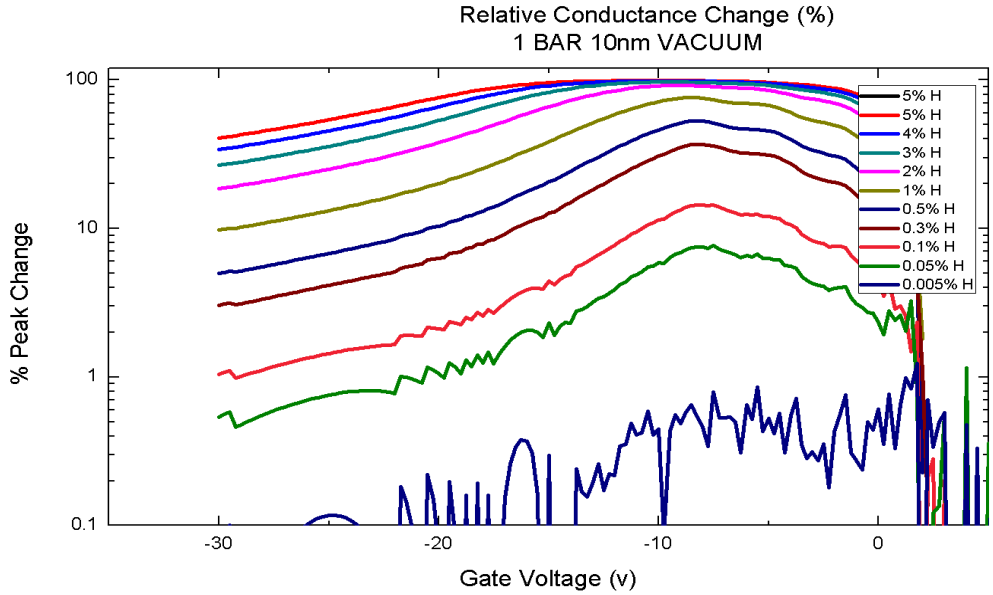

Figure 3.8: Relative Conductance Change (%) of 75nm nanowire at different concentration of H_2 gas when H_2 is exposed in vacuum ambient

Figure 3.8 shows the relative conductance change (%) of 58µm long p-type Si NWs for 10nm nanowire thickness in vacuum ambient at different concentration of H_2 with pressure of hydrogen gas 1bar. If we focused on the figure the peak change (%) is almost at -10.0v gate voltage in vacuum ambient. Peak % change for 5% H_2 is 99.168215 whereas for 0.005% is 0.445826522.

For 10 nm if we look at the peak change from air to vacuum, here the SINW is more sensitive to vacuum ambient.

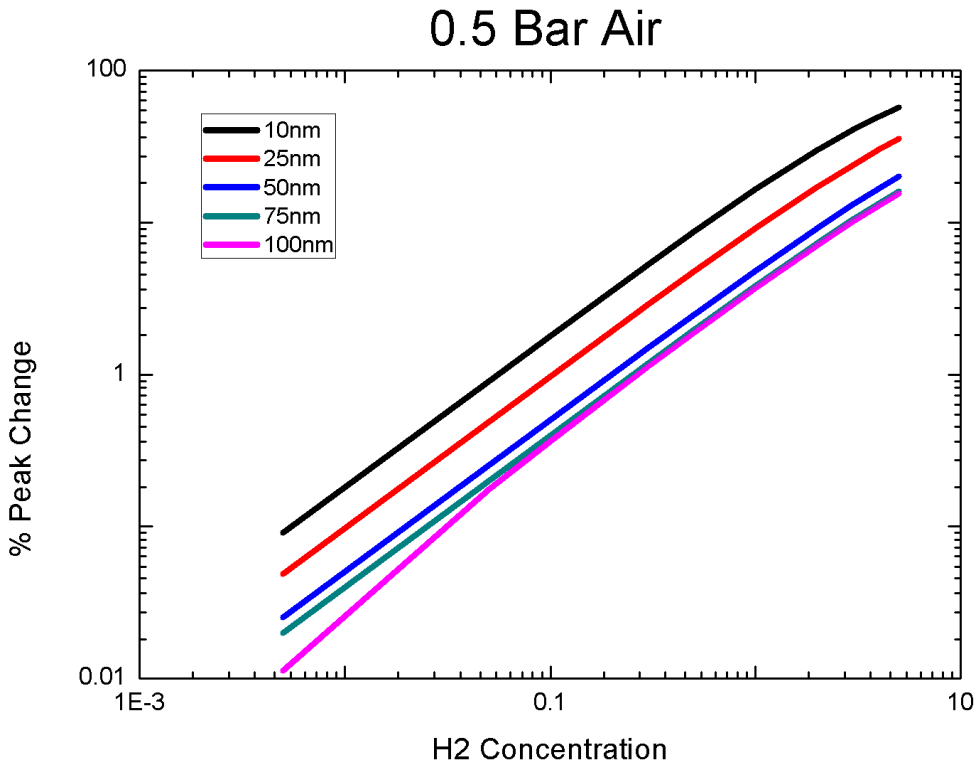

Figure 3.9(a): Peak conductance change (%) with respect to air as a function of H_2 concentration for nanowire with different thicknesses and for H_2 concentration at 0.5 bar pressure

Figure 3.9(a) shows the peak conductance change as a function of the hydrogen concentration for different thickness of SiNW when H_2 gas pressure was 0.5 bar air. From this curve we can extract the % peak change that will be exhibited by the nanowire at different H_2 concentration.

Relative conductance change is the representative figure of merit that sets the gas sensitivity of sensor. The nano-sensor block tested for gas sensing comprised 58μm long nanowires and 30 nanowires connected in parallel had a base current of 1.3nA at VGS=-0.75 V (peak conductance change point) and 1% conductance change corresponds to a 13pA change in current. Agilent B1500A Semiconductor Parameter Analyser is being used here for characterizing electrical response of our nanowires at different ambient are capable of detecting even fA level of current. This can be set in differential mode where sensor response with targeted gas exposure is compared with sensor response in air to display the relative change in current and, hence we set 1% relative conductance change as our lowest detection limit. [11]

Setting the detection limit at 1% it is found that it can detect 0.05% (500ppm) H_2 gas for thickness of 10 nm and can detect 0.25% (2500ppm) H_2 gas for 100 nm thickness of nanowire.

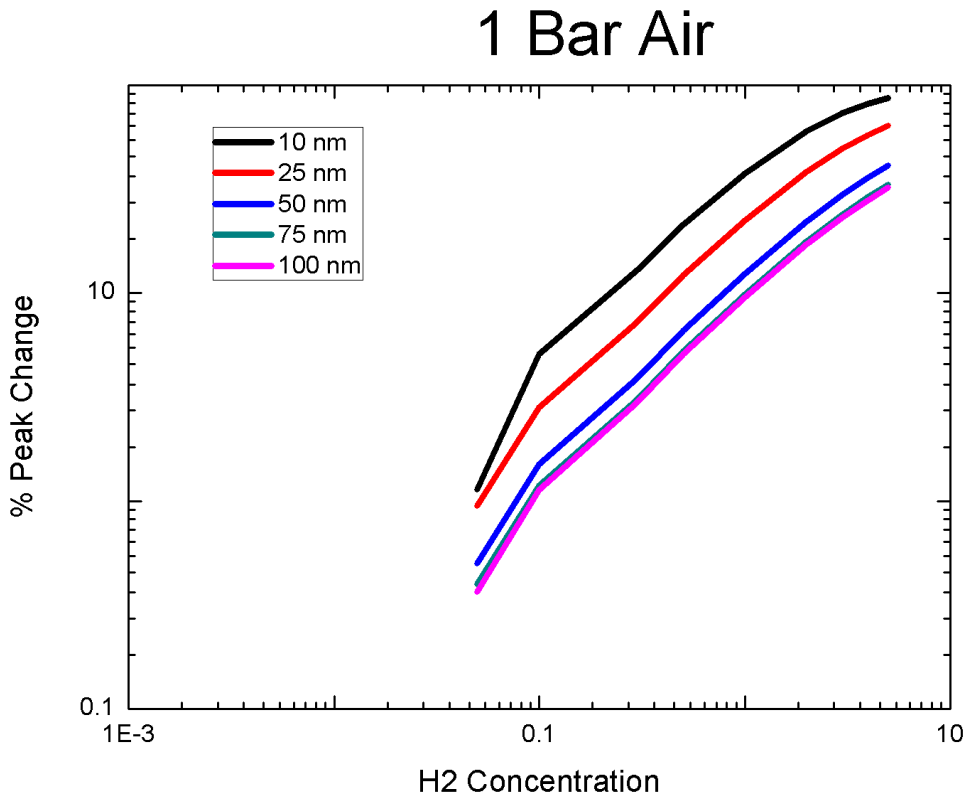

Figure 3.9(b): Peak conductance change (%) with respect to air as a function of H_2 concentration for nanowire with different thicknesses and for H_2 concentration at 1.0 bar pressure

Figure 3.9(b) shows the peak conductance change as a function of the hydrogen concentration for different thickness of SiNW when H_2 gas pressure was 1.0 bar air. From this curve we can extract the % peak change that will be exhibited by the nanowire at different H_2 concentration.

Setting the detection limit at 1% it is found that it can detect 0.04% (400ppm) H_2 gas for thickness of 10 nm and can detect 0.08% (800ppm) H_2 gas for 100 nm thickness of nanowire.

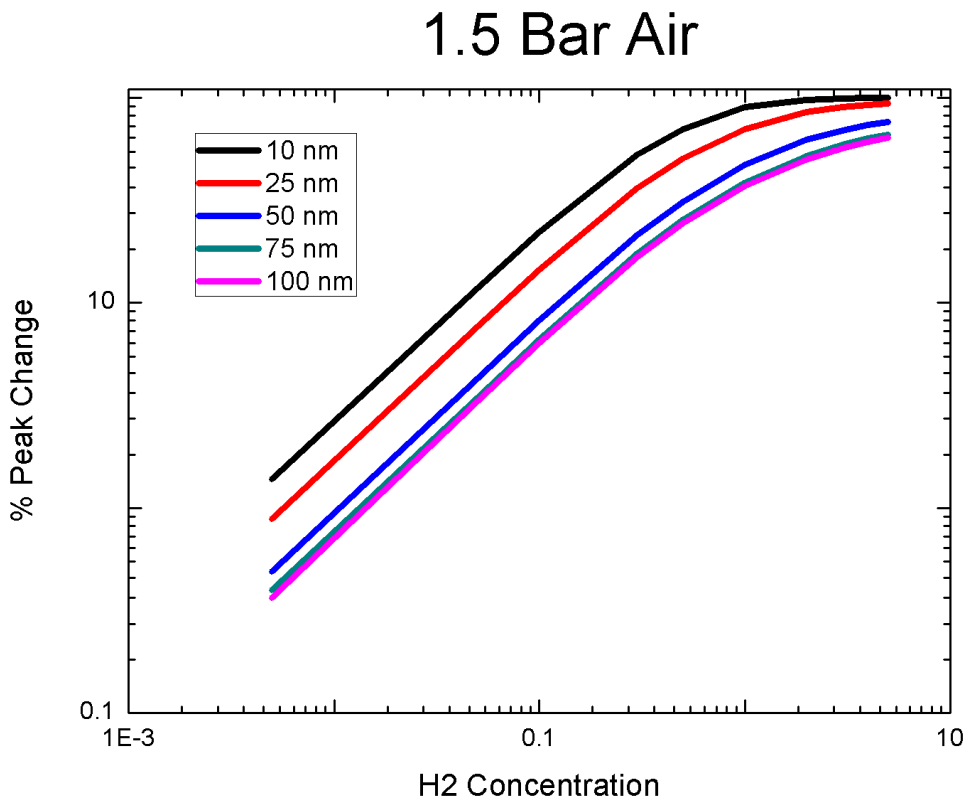

Figure 3.9(c): Peak conductance change (%) with respect to air as a function of H_2 concentration for nanowire with different thicknesses and for H_2 concentration at 1.5 bar pressure

Figure 3.9(c) shows the peak conductance change as a function of the hydrogen concentration for different thickness of SiNW when H_2 gas pressure was 1.5 bar air. From this curve we can extract the % peak change that will be exhibited by the nanowire at different H_2 concentration.

Setting the detection limit at 1% it is found that it can detect H_2 gas down to 0.005% (50ppm) for thickness of 10 nm and can detect 0.01% (100ppm) H_2 gas for 100 nm thickness of nanowire.

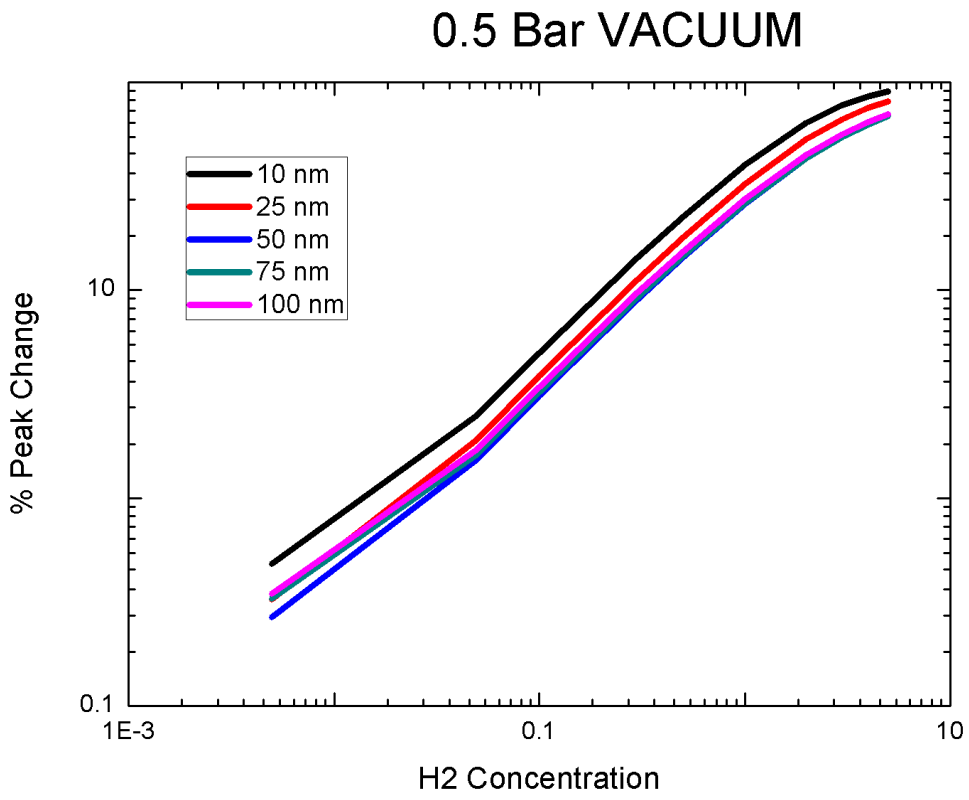

Figure 3.10(a): Peak conductance change (%) with respect to vacuum as a function of H_2 concentration for nanowire with different thicknesses and for H_2 concentration at 0.5 bar pressure

Figure 3.10(a) shows the peak conductance change as a function of the hydrogen concentration for different thickness of SiNW when H_2 gas pressure was 0.5 bar vacuum pressure. From this curve we can extract the % peak change that will be exhibited by the nanowire at different H_2 concentration.

It can be seen that when H_2 gas is exposed in vacuum ambient SiNW become more sensitive. For 100nm thickness it can detect down to 0.02% (200ppm) gas where for 10nm thickness it can detect down to 0.01% (100ppm) gas.

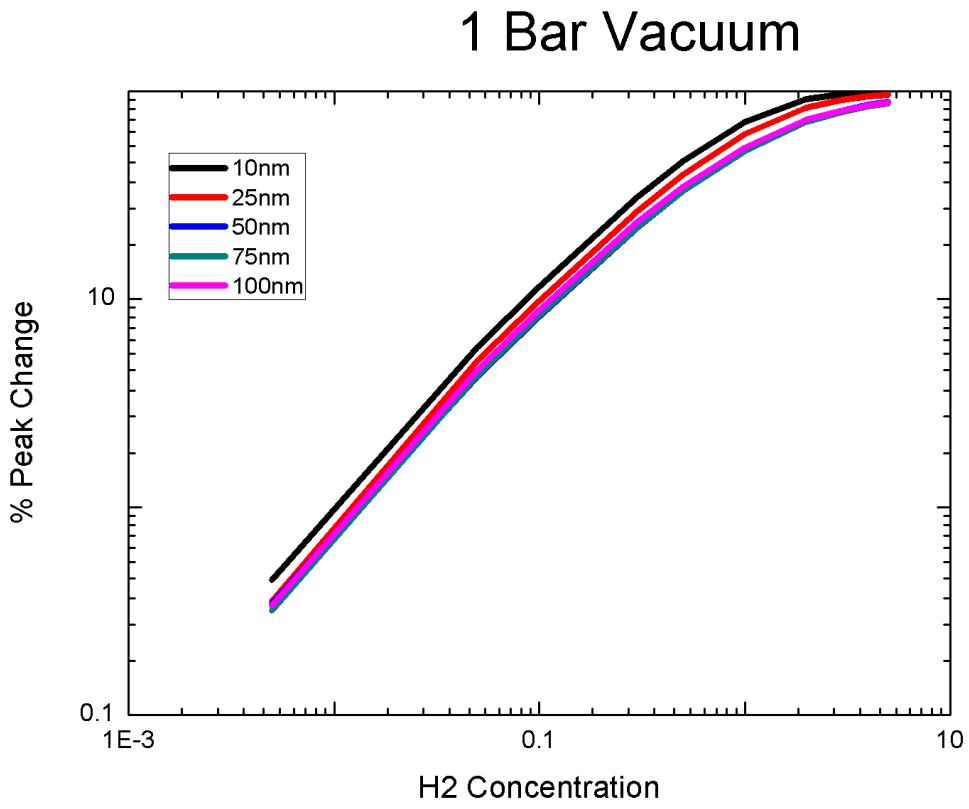

Figure 3.10(b): Peak conductance change (%) with respect to vacuum as a function of H_2 concentration for nanowire with different thicknesses and for H_2 concentration at 1.0 bar pressure

Figure 3.10(b) shows the peak conductance change as a function of the hydrogen concentration for different thickness of SiNW when H_2 gas pressure was 1.0 bar vacuum pressure. From this curve we can extract the % peak change that will be exhibited by the nanowire at different H_2 concentration.

For 100nm thickness it can detect down to 0.01% (100ppm) gas where for 10nm thickness it can detect down to 0.01% (100ppm) gas.

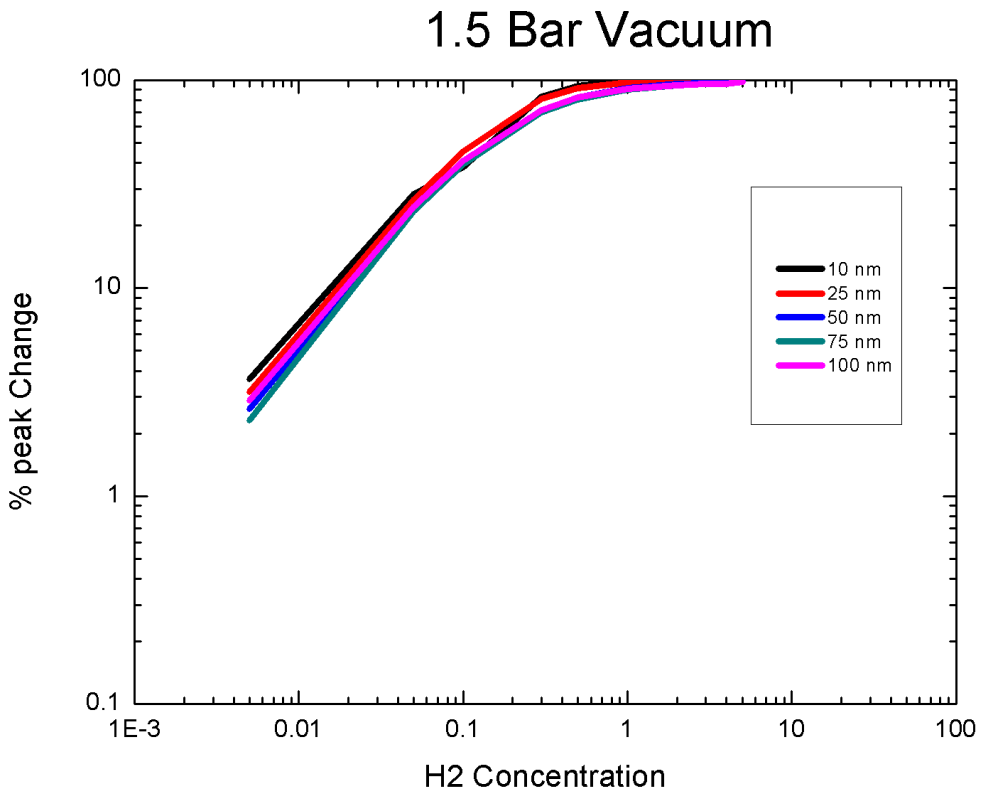

Figure 3.10(c): Peak conductance change (%) with respect to vacuum as a function of H_2 concentration for nanowire with different thicknesses and for H_2 concentration at 1.5 bar pressure

Figure 3.10(c) shows the peak conductance change as a function of the hydrogen concentration for different thickness of SiNW when H_2 gas pressure was 1.5 bar vacuum pressure. From this curve we can extract the % peak change that will be exhibited by the nanowire at different H_2 concentration.

For 100nm thickness it can detect below 0.005% (50ppm) gas where for 10nm thickness it can detect below 0.005% (50ppm) gas.

For 1% peak change in air ambient the lowest concentration of H_2 is detected by 1.5 bar at 10nm in air ambient which is below 0.005% (50ppm). For vacuum the lowest concentration of H_2 is also detected by 1.5 bar which is also below 0.005% (50ppm). If we analysis the concentration of gas that is detected by air and vacuum in different pressure we can say that the vacuum can sense lowest concentration of hydrogen gas than air. It is also can figured out that if the thickness of SiNW is decreased it detect lower concentration of gas for a particular pressure.

Chapter 4

Conclusion

In this work we investigated feasibility of SiNW for hydrogen gas sensing application. We used here a p-type SiNW of 58μm long to sense H_2 gas. The source and drain doping was $10^{20}/cm^3$ and body doping was $6 \times 10^{16}/cm^3$. This particular structure used to resemble fabricated NW platform that had been used to extract the surface states density of SiNW when exposure of H_2 gas with pressure of 0.5, 1.0 and 1.5 bar. We found that 100nm thick SiNW can exhibit sensitivity of H_2 gas down to 2500 ppm, 800 ppm, and 100 ppm for pressures of 0.5, 1.0 and 1.5 bar respectively if H_2 is exposed on NW in natural ambient. If H_2 is exposed on NW in vacuum environment this sensitivity goes down to 200 ppm, 100 ppm, and below 50 ppm respectively for 0.5, 1.0 and 1.5 bar. With the reduction of NW thickness a significant improvement of H_2 sensitivity was observed. For 10nm thickness SiNW exhibited sensitivity of H_2 gas down to 500 ppm, 400 ppm, and below 50 ppm for pressure of 0.5, 1.0 and 1.5 bar respectively in natural ambient and in vacuum environment this sensitivity goes down to 100 ppm, 100 ppm, and below 50 ppm respectively for 0.5, 1.0 and 1.5 bar.

References

1. A. Cao, E. Sudhölter, and L. D. Smet, "Silicon Nanowire-Based Devices for Gas-Phase Sensing," Sensors, vol. 14, no. 1, pp. 245–271, 2013.
2. "Gas detector," *Wikipedia*, 02-Aug-2018. [Online]. Available: https://en.wikipedia.org/wiki/Gas_detector. [Accessed: 04-Aug-2018].
3. Wenting LI, B. ENG., "The selectivity of UV-light activated metal oxide semiconductor gas sensors manifested by two competing redox processes*."* M.Sc. thesis, McMaster University, Canada, Jun. 2015.
4. "How infrared gas detectors work," *EnggCyclopedia*, 11-Nov-2017. [Online]. Available: http://www.enggcyclopedia.com/2011/11/infrared-gas-detectors/. [Accessed: 04-Aug-2018].
5. S. Mishra, C. Ghanshyam, N. Ram, R. Bajpai, and R. Bedi, "Detection mechanism of metal oxide gas sensor under UV radiation," *Sensors and Actuators B: Chemical*, vol. 97, no. 2-3, pp. 387–390, 2004.
6. "Gas chromatography," *Wikipedia*, 03-Aug-2018. [Online]. Available: https://en.wikipedia.org/wiki/Gas_chromatography. [Accessed: 04-Aug-2018].
7. C. Wang, L. Yin, L. Zhang, D. Xiang, and R. Gao, "Metal Oxide Gas Sensors: Sensitivity and Influencing Factors," *Sensors*, vol. 10, no. 3, pp. 2088–2106, 2010.
8. E. Comini and G. Sberveglieri, "Metal oxide nanowires as chemical sensors," *Materials Today*, vol. 13, no. 7-8, pp. 36–44, 2010.
9. Silvaco international, Atlas User's Manual Device Simulation Software, Silvaco International Ltd., Santa Clara, Apr 2010.
10. P. Walker, H. Mizuta, S. Uno, Y. Furuta and D. Hasko, "Improved off-current and subthreshold slope in aggressively scaled poly-Si TFTs with single grain boundary in the channel", IEEE Trans. On Electron Devices, vol. 51, pp. 212-219, 2004.
11. Hakim MMA, Tanzeem S, Sun K and Ashburn P, "Low Cost Mass Manufacturable Silicon Nano-Sensors for Detection of Molecules in Gas Phase*." SF Journal of Nanochemistry and Nanotechnology*, vol. 01, pp. 1-26, 08 Jun. 2018.

Appendix A

Relative Conductance Change

10nm 0.5 Bar AIR:

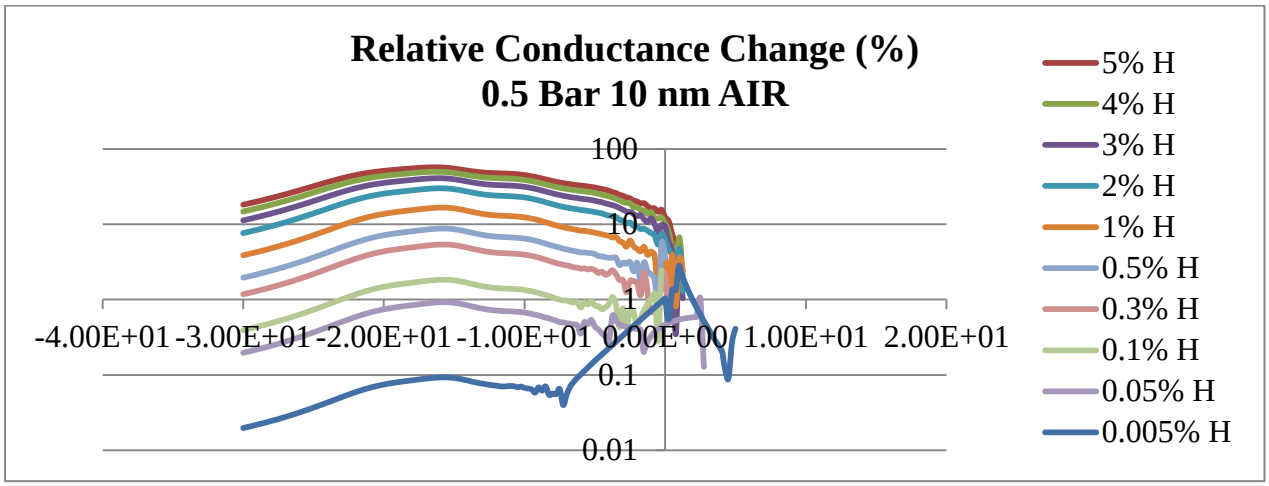

10nm 1 Bar AIR:

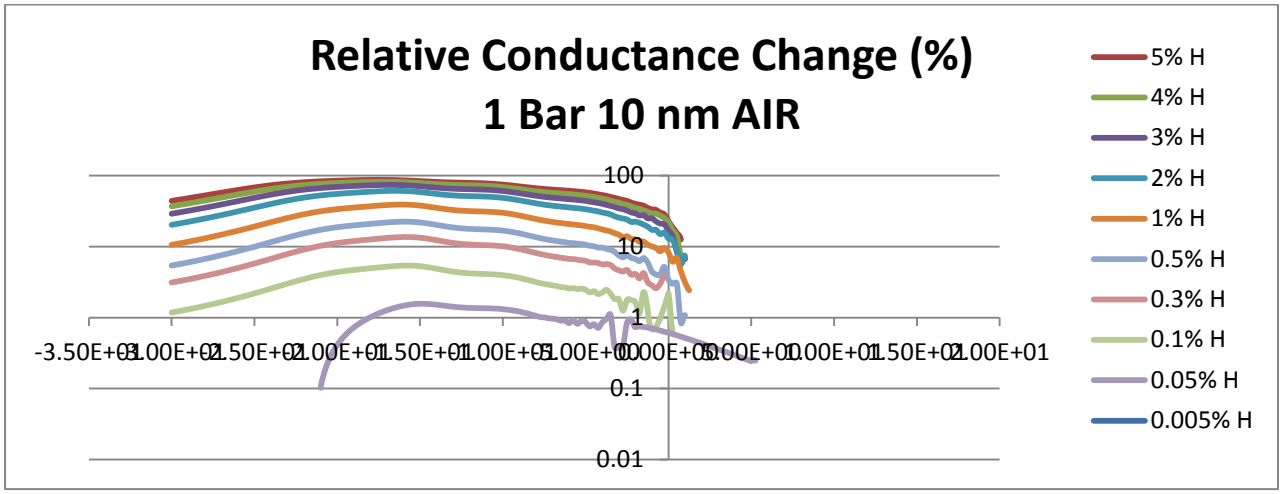

10nm 1.5 Bar AIR:

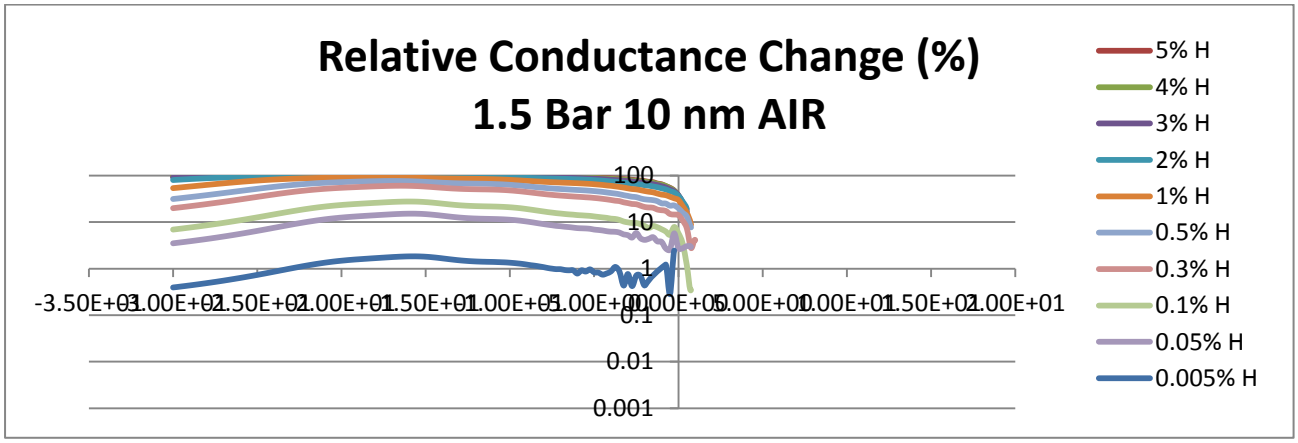

25nm 0.5 Bar AIR:

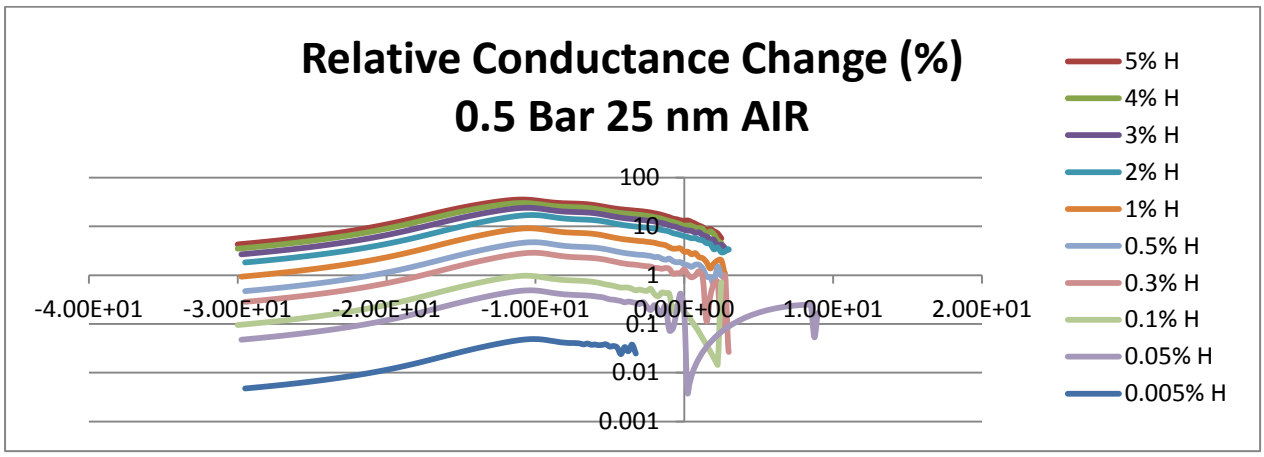

25nm 1 Bar AIR:

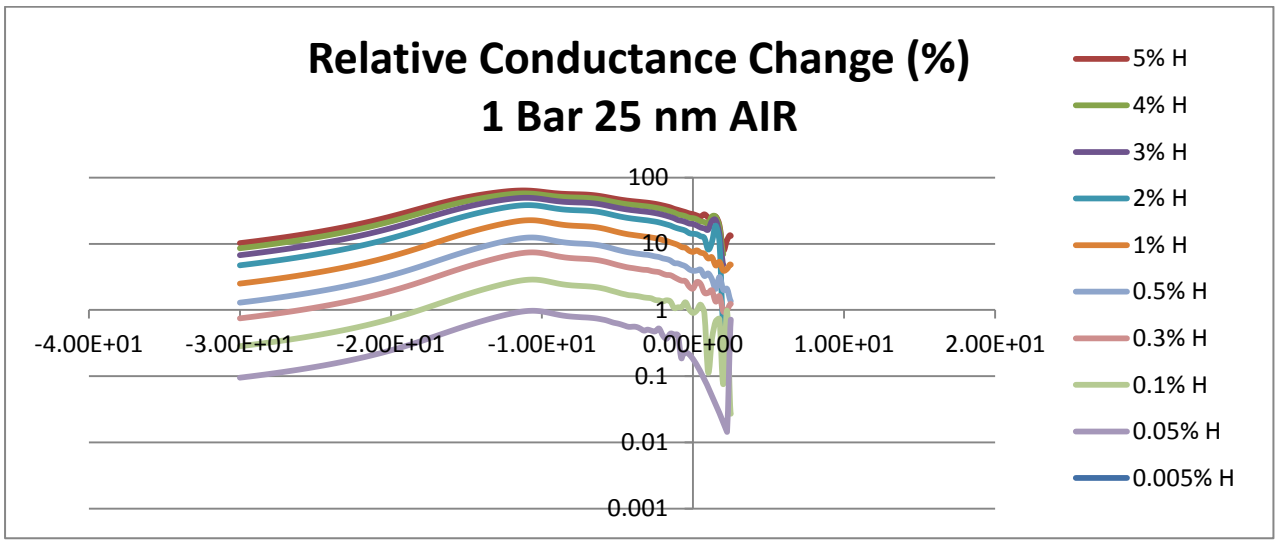

25nm 1.5 Bar AIR:

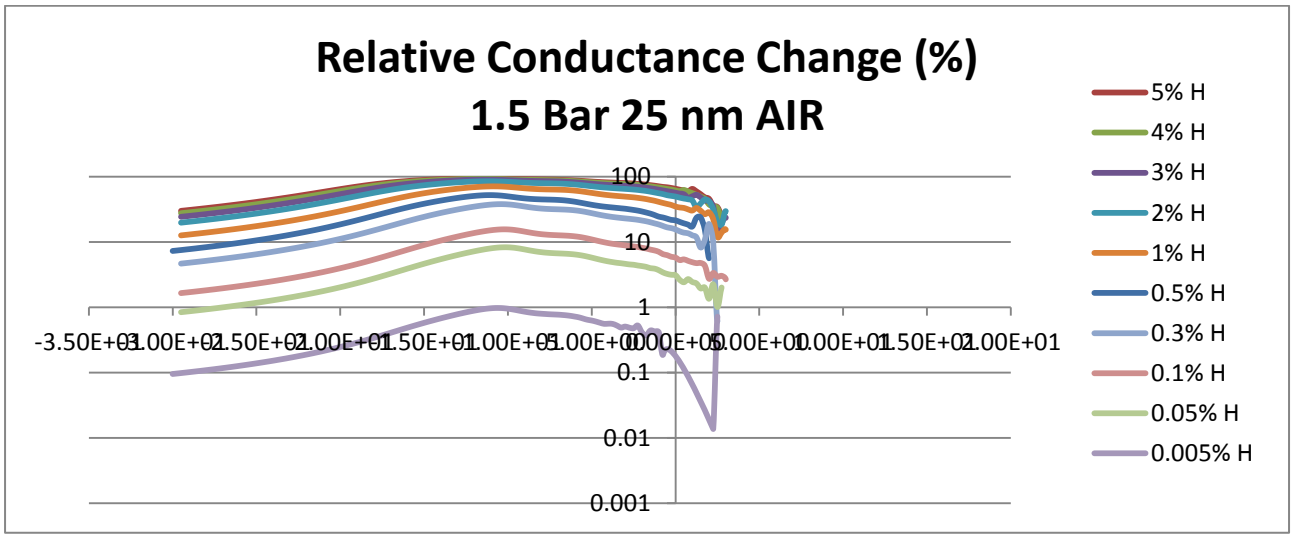

50nm 0.5 Bar AIR:

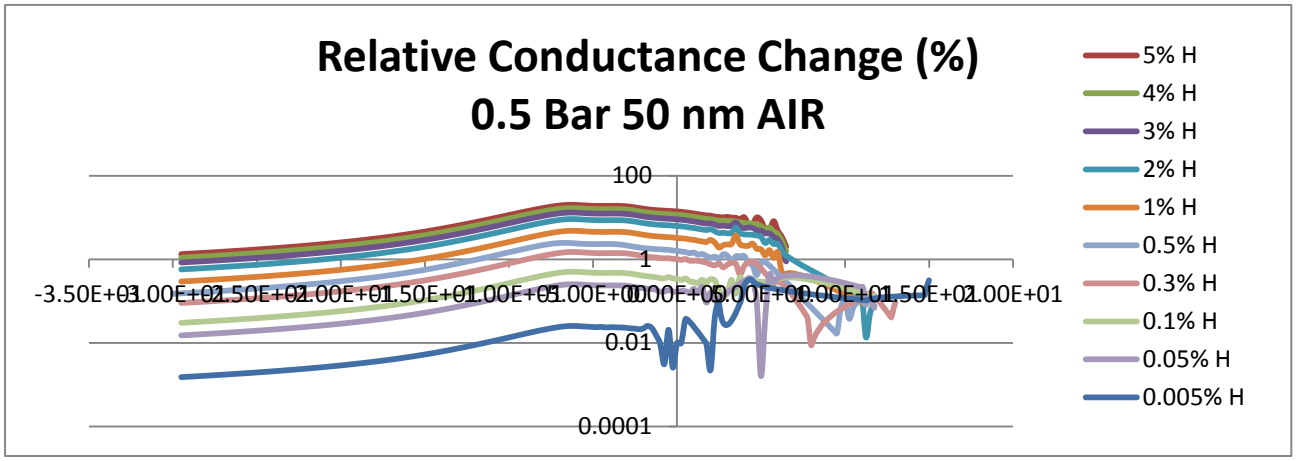

50nm 1 Bar AIR:

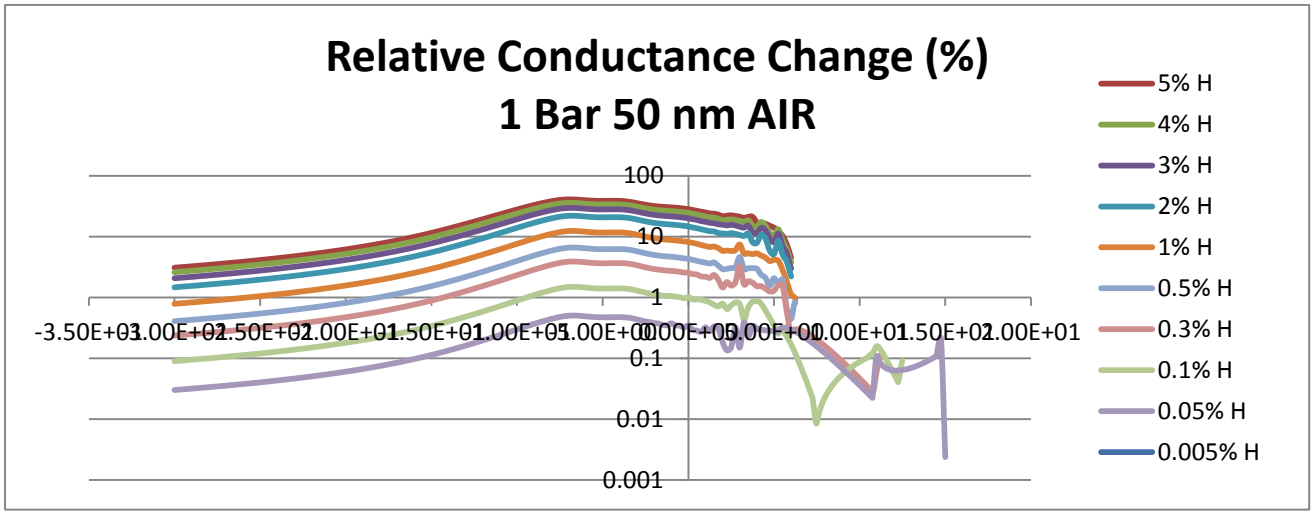

50nm 1.5 Bar AIR:

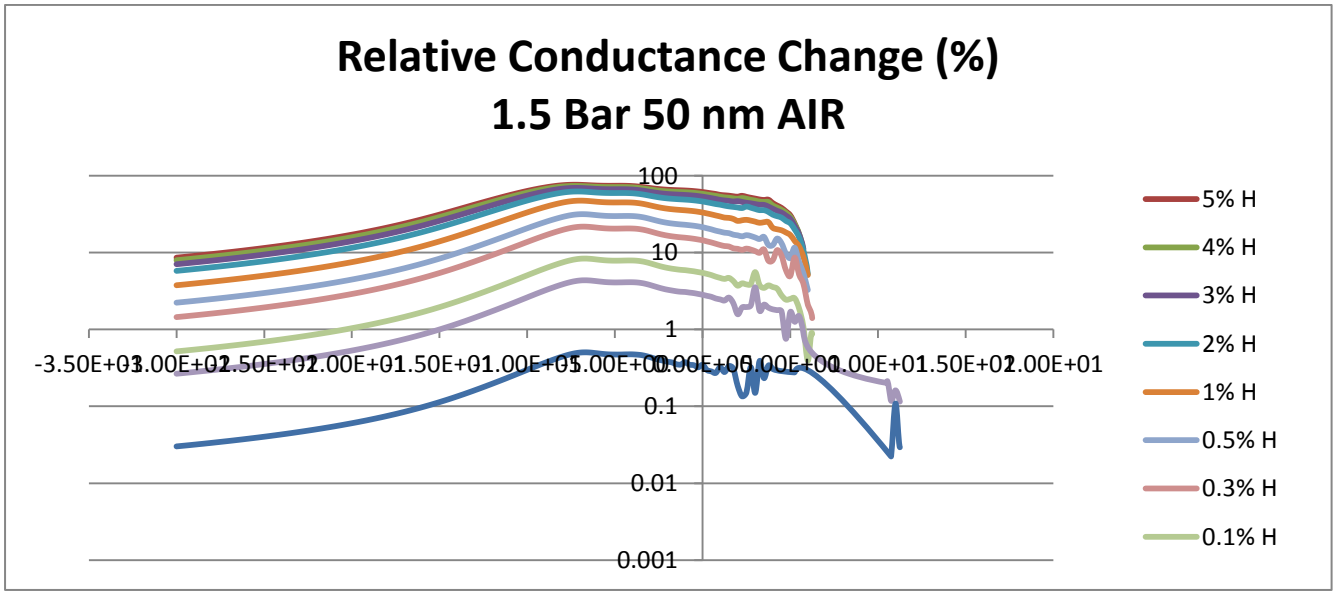

75nm 0.5 Bar AIR:

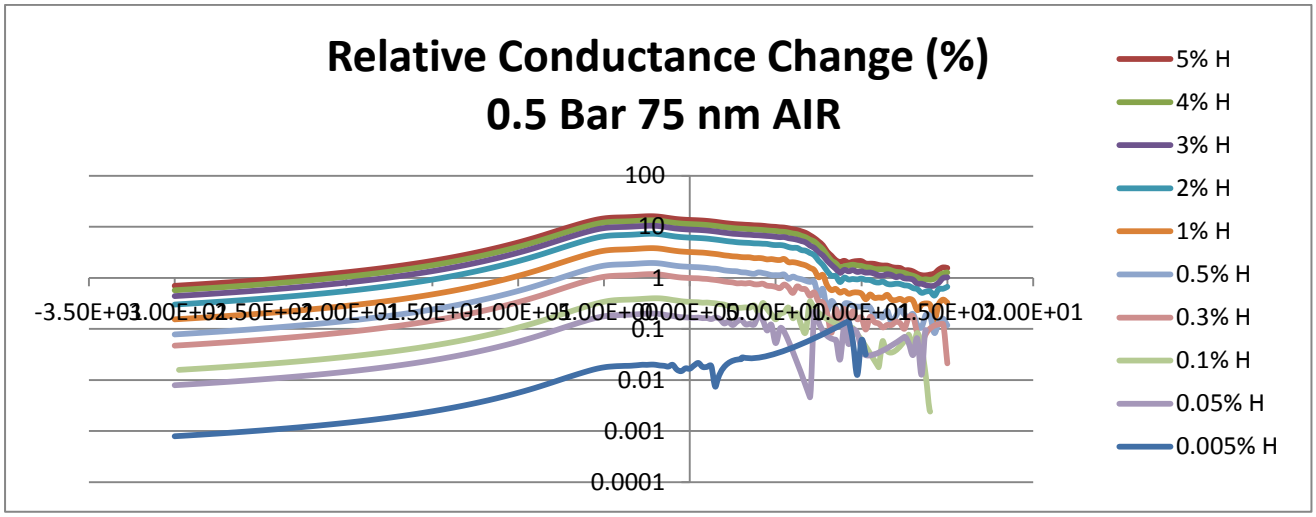

75nm 1 Bar AIR:

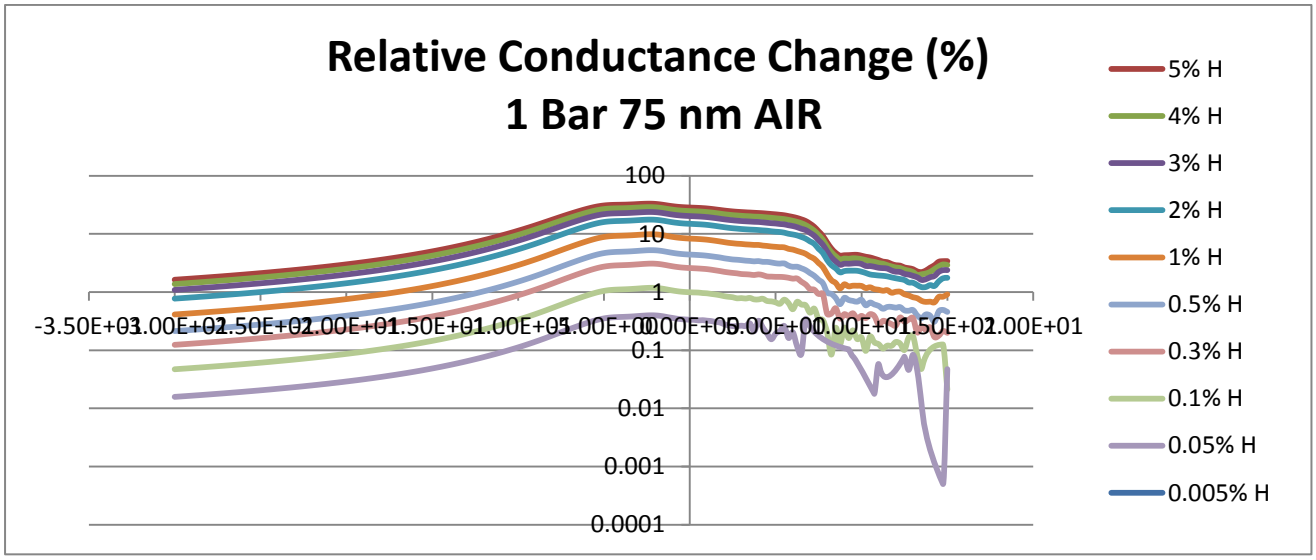

75nm 1.5 Bar AIR:

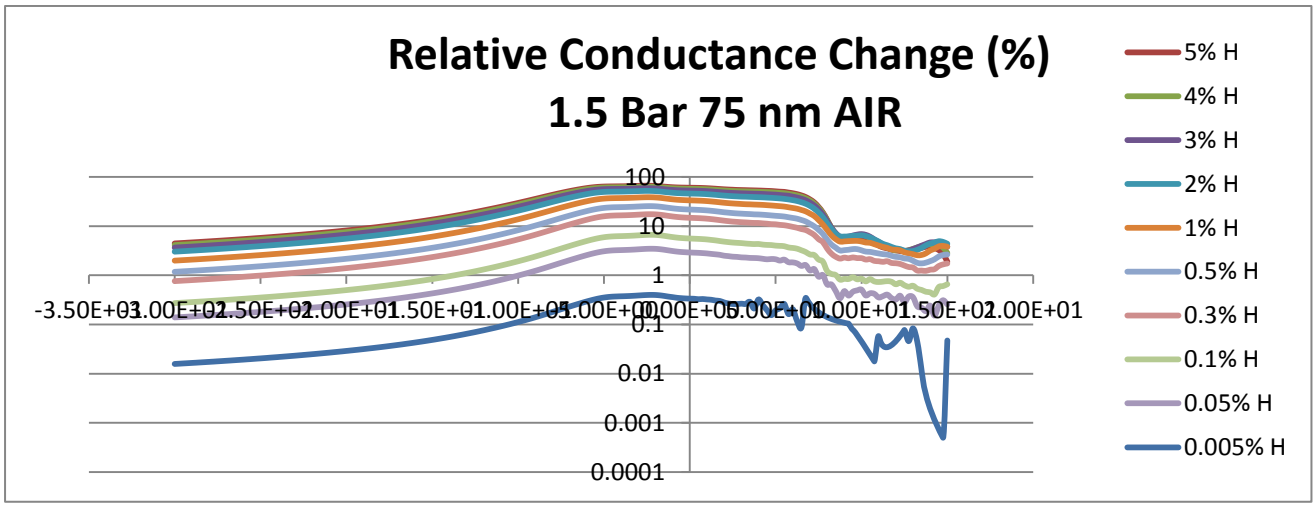

100nm 0.5 Bar AIR:

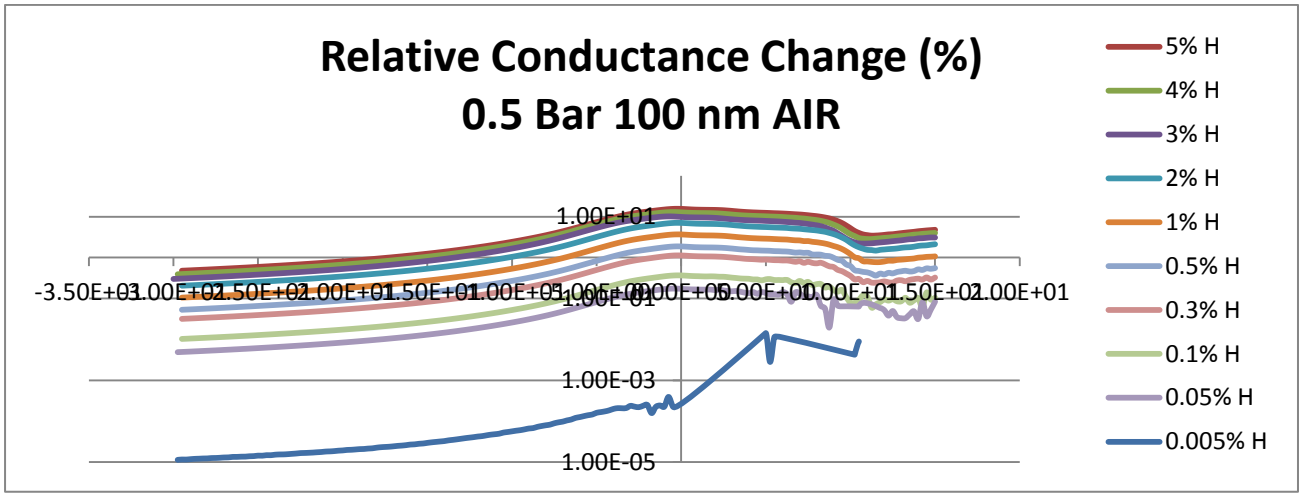

100nm 1 Bar AIR:

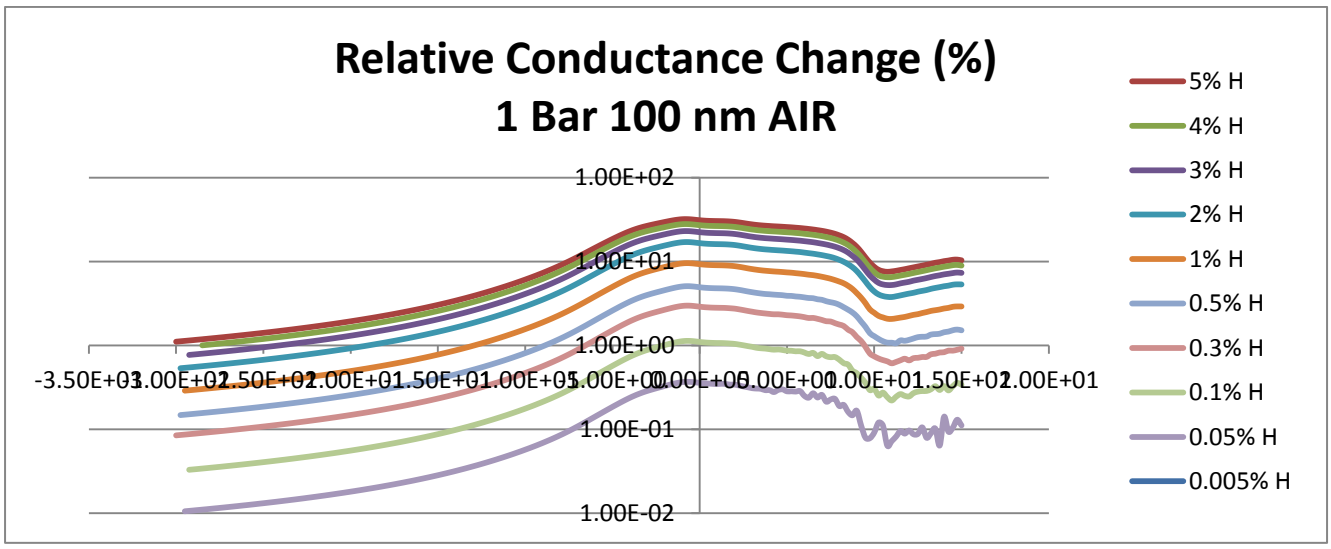

100nm 1.5 Bar AIR:

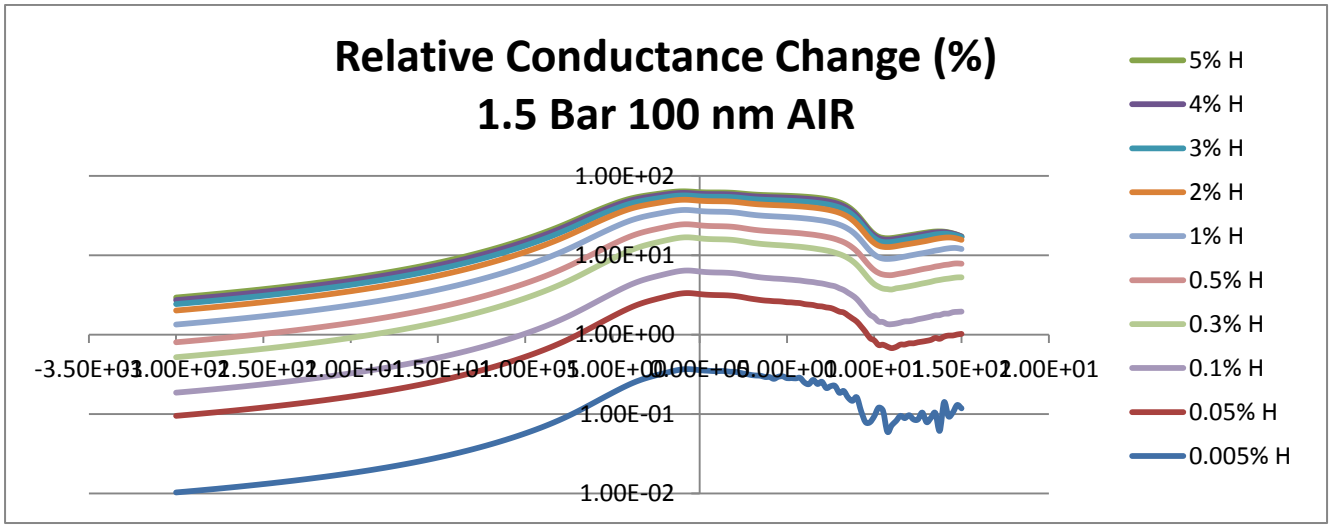

10nm 0.5 Bar VACUUM:

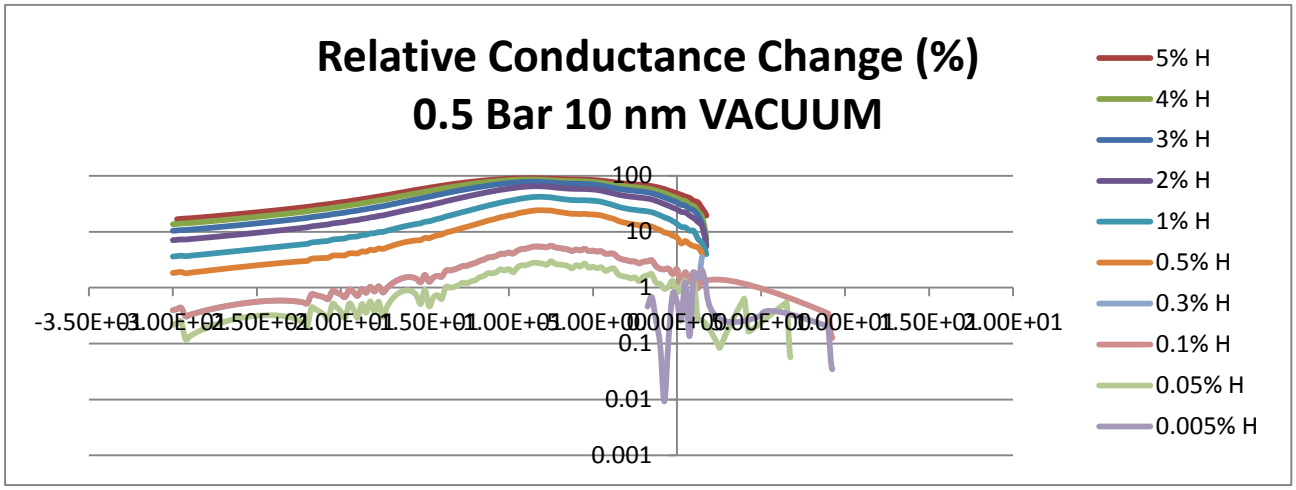

10nm 1 Bar VACUUM:

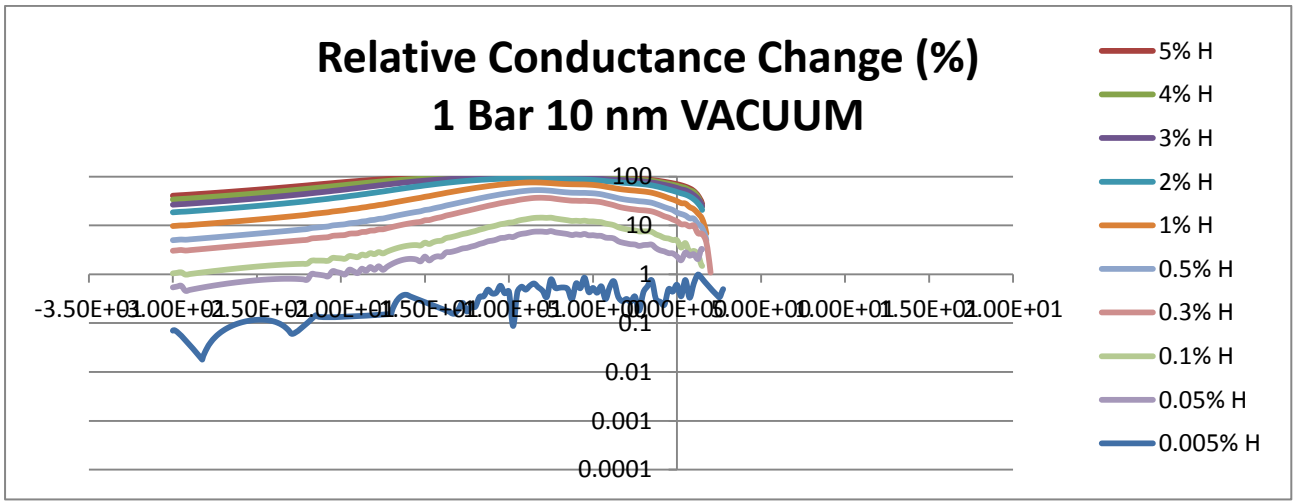

10nm 1.5 Bar VACUUM:

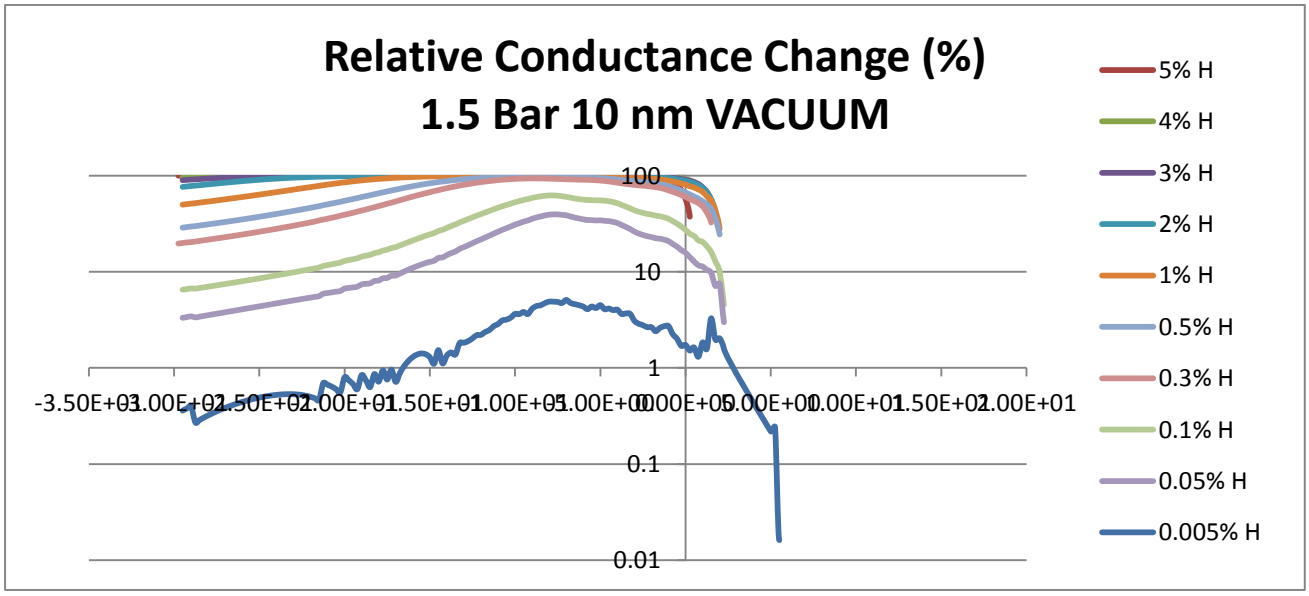

25nm 0.5 Bar VACUUM:

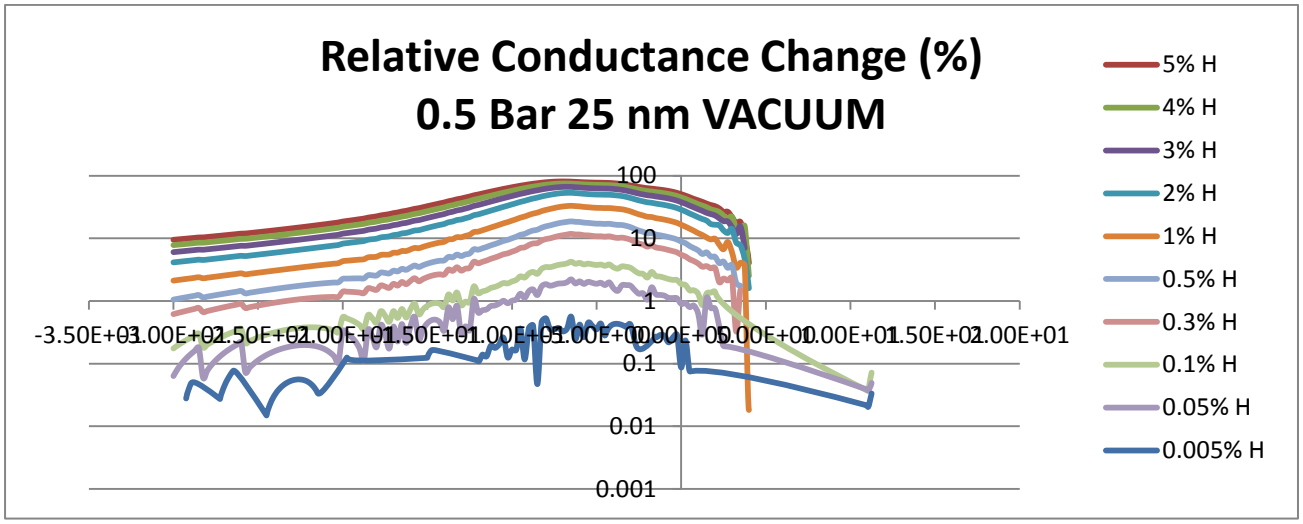

25nm 1 Bar VACUUM:

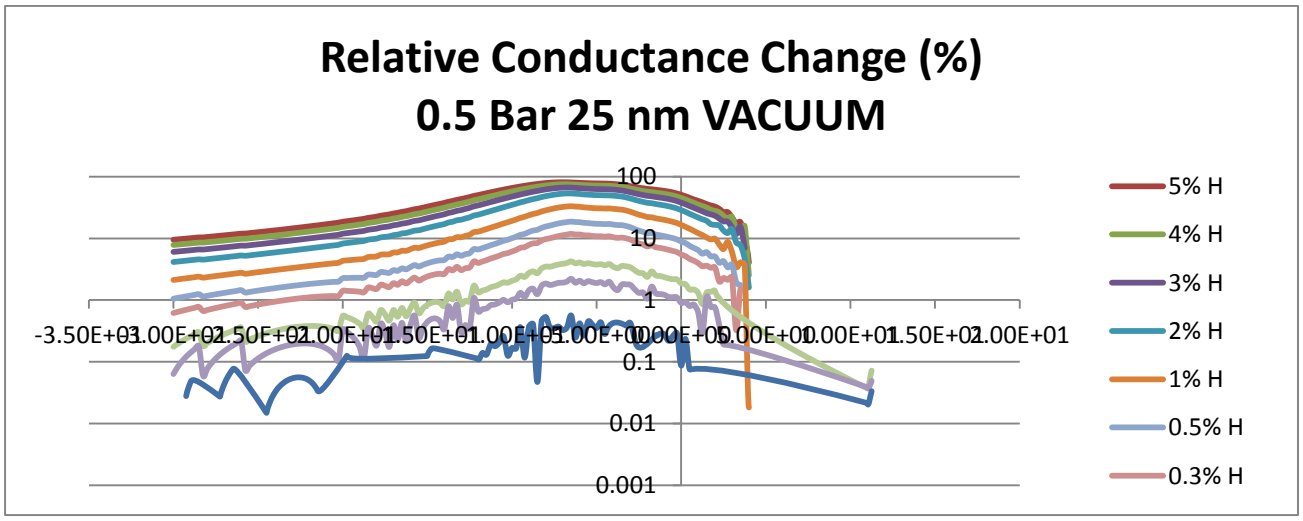

25nm 1.5 Bar VACUUM:

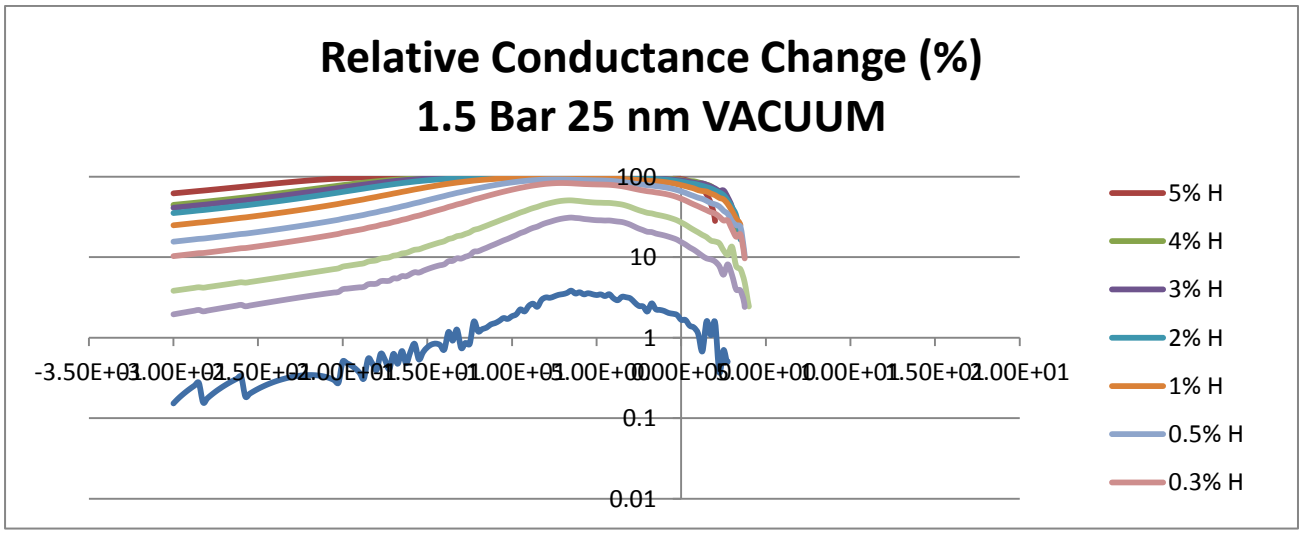

50nm 0.5 Bar VACUUM:

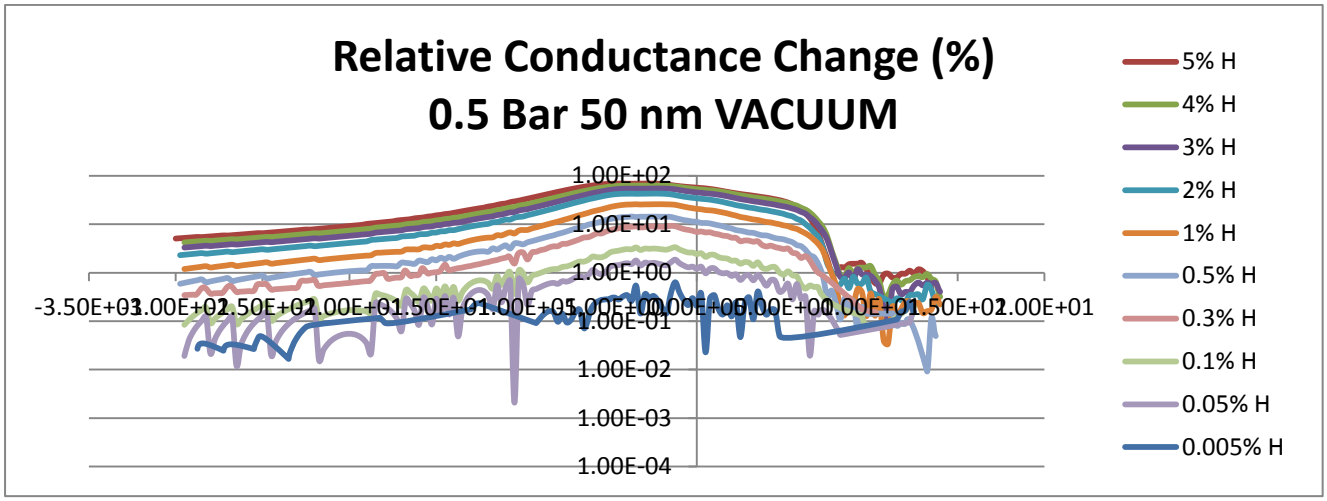

50nm 1 Bar VACUUM:

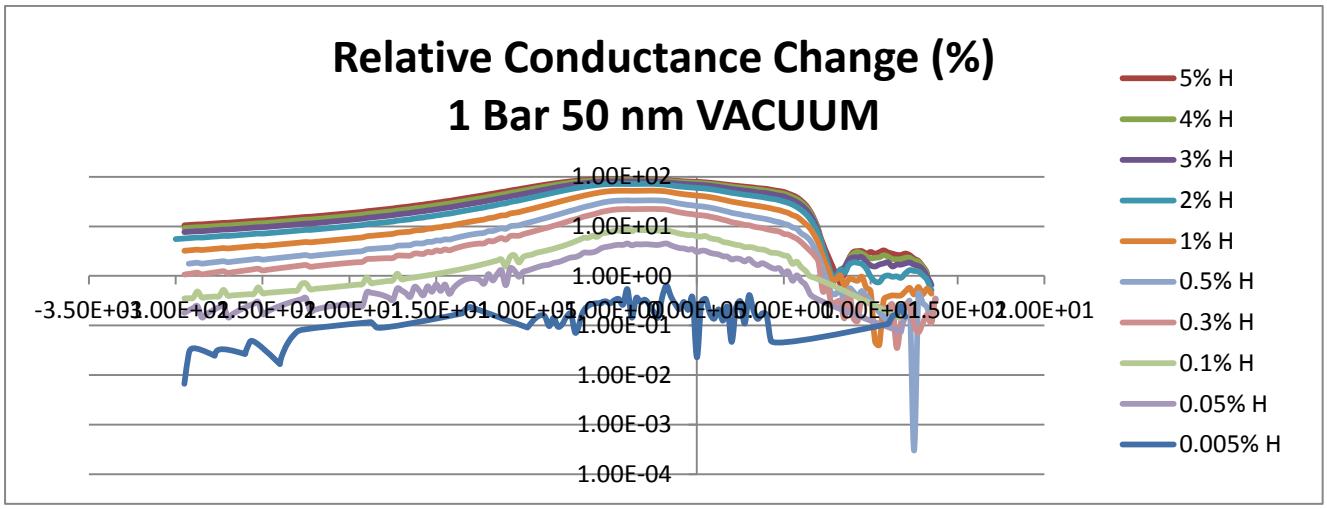

50nm 1.5 Bar VACUUM:

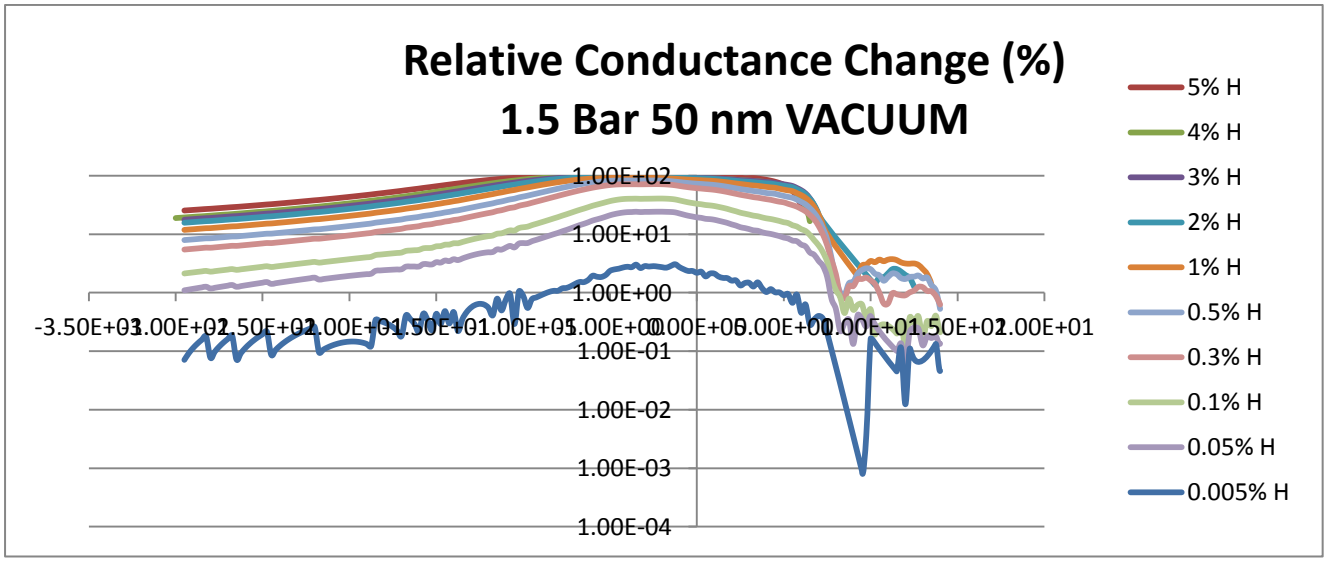

75nm 0.5 Bar VACCUM:

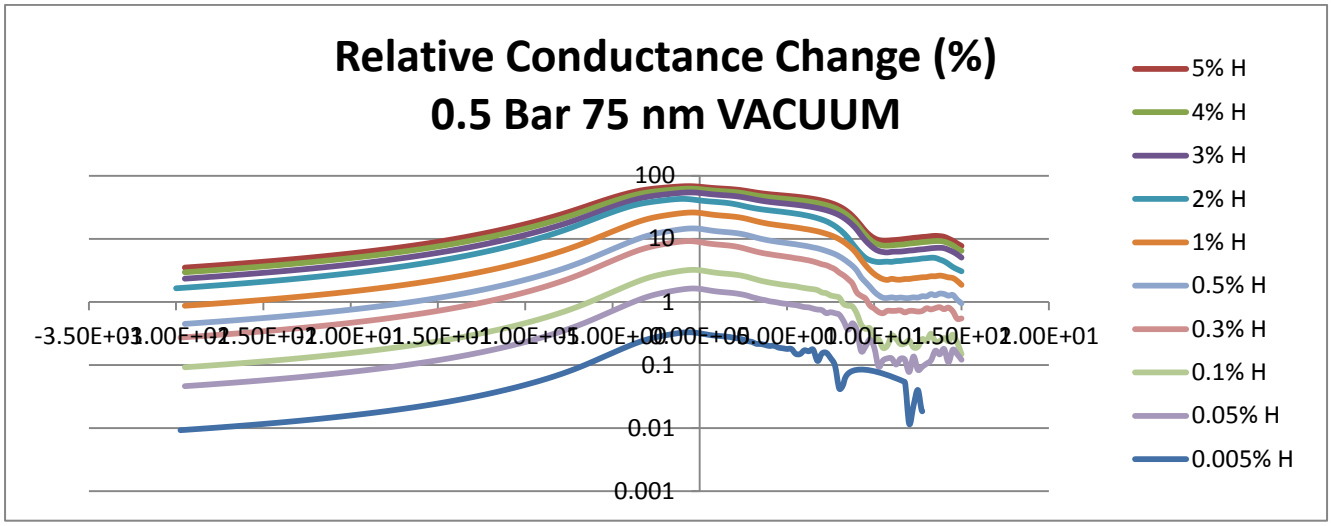

75nm 1 Bar VACCUM:

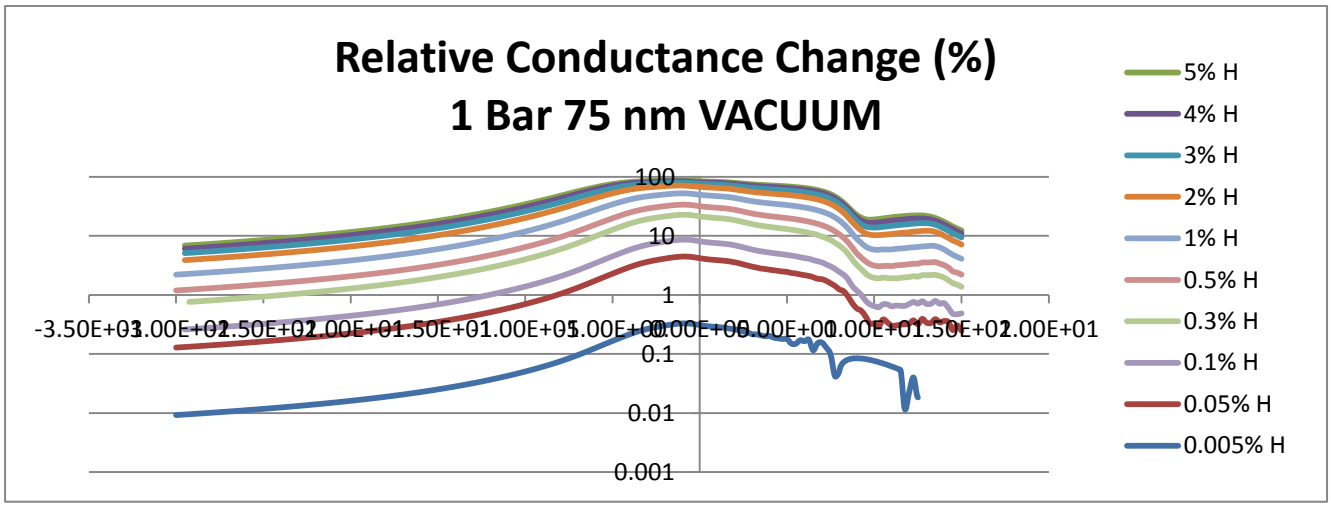

75nm 1.5 Bar VACCUM:

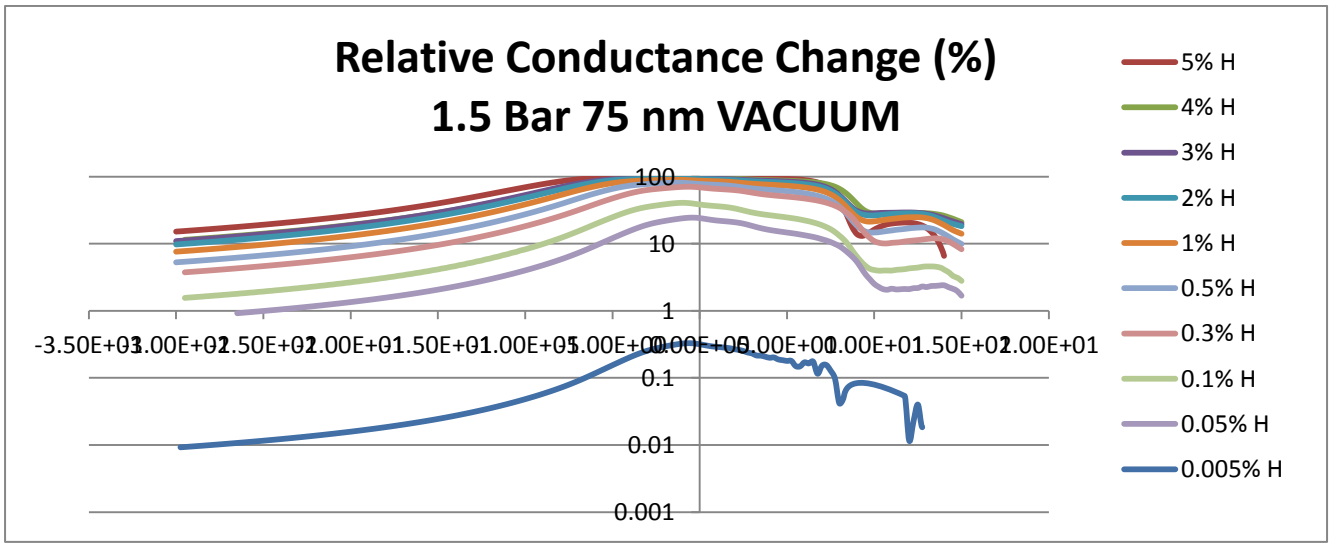

100nm 0.5 Bar VACUUM:

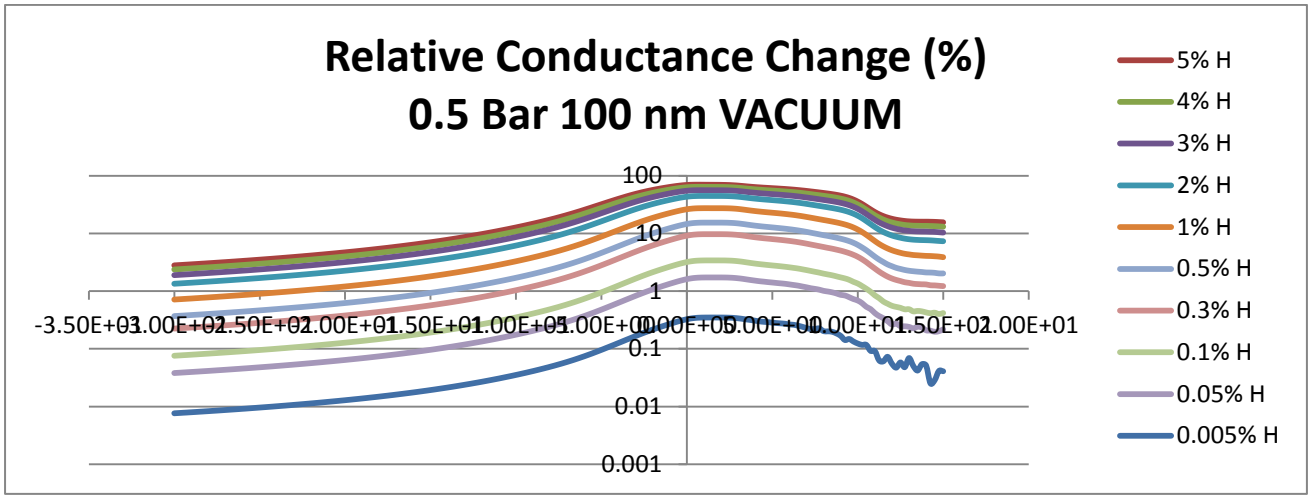

100nm 1 Bar VACUUM:

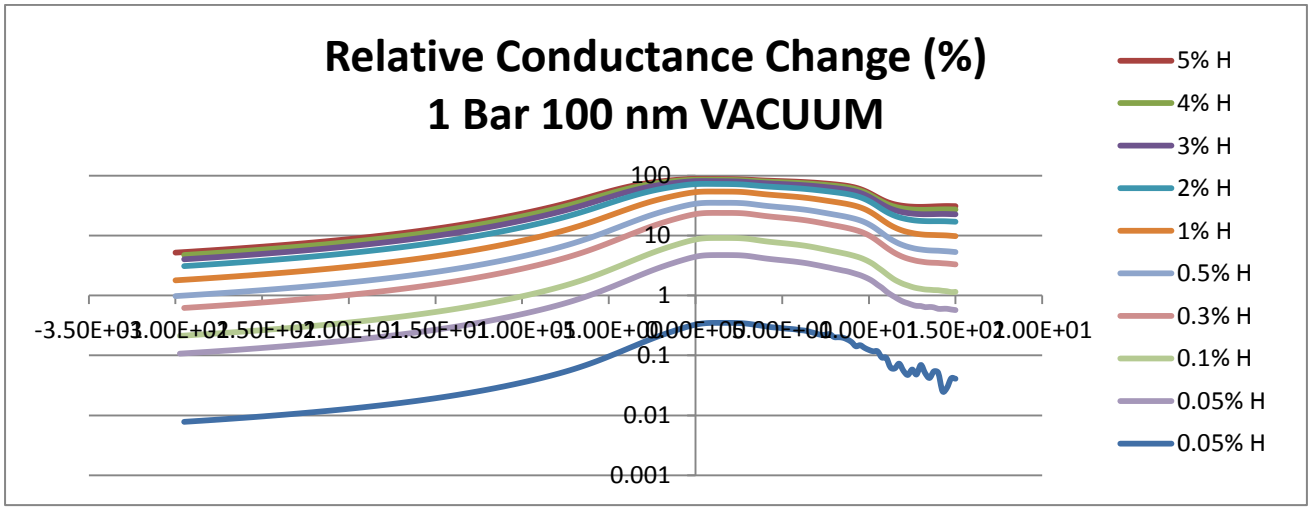
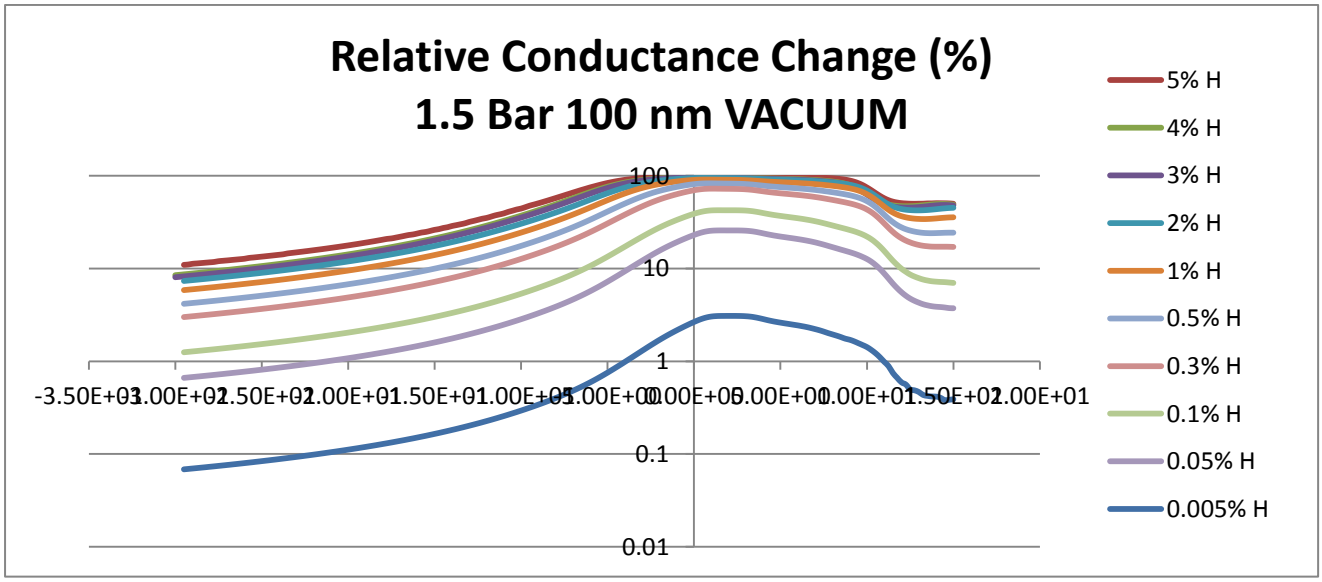
100nm 1.5 Bar VACUUM: